

# Holevo Cramér-Rao bound: How close can we get without entangling measurements?

Aritra Das,<sup>1,\*</sup> Lorcán O. Conlon,<sup>2</sup> Jun Suzuki,<sup>3</sup> Simon K. Yung,<sup>1,2</sup> Ping K. Lam,<sup>2,1</sup> and Syed M. Assad<sup>2,1</sup>

<sup>1</sup>*Centre for Quantum Computation and Communication Technology, Department of Quantum Science and Technology, Australian National University, Canberra, ACT 2601, Australia*

<sup>2</sup>*A\*STAR Quantum Innovation Centre (Q.InC), Institute of Materials Research and Engineering (IMRE), Agency for Science, Technology and Research (A\*STAR), 2 Fusionopolis Way, 08-03 Innovis 138634, Singapore*

<sup>3</sup>*Graduate School of Informatics and Engineering, The University of Electro-Communications, 1-5-1 Chofugaoka, Chofu-shi, Tokyo 182-8585, Japan*

(Dated: May 16, 2024)

In multi-parameter quantum metrology, the resource of entanglement can lead to an increase in efficiency of the estimation process. Entanglement can be used in the state preparation stage, or the measurement stage, or both, to harness this advantage—here we focus on the role of entangling measurements. Specifically, entangling or collective measurements over multiple identical copies of a probe state are known to be superior to measuring each probe individually, but the extent of this improvement is an open problem. It is also known that such entangling measurements, though resource-intensive, are required to attain the ultimate limits in multi-parameter quantum metrology and quantum information processing tasks. In this work we investigate the maximum precision improvement that collective quantum measurements can offer over individual measurements for estimating parameters of qudit states, calling this the ‘collective quantum enhancement’. We show that, whereas the maximum enhancement can, in principle, be a factor of  $n$  for estimating  $n$  parameters, this bound is not tight for large  $n$ . Instead, our results prove an enhancement linear in dimension of the qudit is possible using collective measurements and lead us to conjecture that this is the maximum collective quantum enhancement in any local estimation scenario.

## I. INTRODUCTION

Over half-a-century of advances in quantum metrology [1–3] has vastly improved our ability to measure, sense, image, and estimate with enhanced precision [4–9]. Of significant interest is the multi-parameter estimation scenario [3, 10–13], where two hall-mark quantum effects manifest themselves, playing opposing roles. On the one hand, quantum incompatibility between the unknown parameters [14–17] hinders their simultaneous measurement from a single copy of an unknown state [3, 18]. On the other hand, given multiple identical copies of the state, an entangling measurement on all the copies, called a collective (or joint) measurement [19], can extract more information about the parameters than any measurement where the copies are measured individually<sup>1</sup> [20–22]. As individual and separable measurements can be recovered as special cases of collective measurements, it is clear that the latter can only lead to precision enhancements in estimation tasks [22, 23], but the extent of this improvement is a major open problem [21, 24]. In this work, we study *the maximum enhancement collective measurements stand to offer over individual measurements*, specifically in the context of parameter estimation and state tomography.

Despite their advantages, collective measurements are challenging to implement in any real estimation scenario

and experimental demonstrations are few and far between [22, 23, 25–27]. Resultantly, the ratio between the optimal precisions attainable via collective versus individual measurement serves as a useful quantifier of both the quantum advantage offered by collective measurements, and the utility of performing complicated entangling measurements and expending vast amounts of resources. If this ratio is small, then there is not much advantage to be gained from entangling measurements. But even if the ratio is large, our ability to perform the requisite measurements might be limited, meaning that the collective performance is just an overly optimistic goal that is far from being achievable.

Collective measurements are known to not offer any advantage for estimating a single parameter [1] or multiple parameters of a pure state [28]. Beyond this, except for some simple cases, not much is known about the optimal individual or collective measurement strategies or their performance relative to each other. One reason for this is that the analytic evaluation of the optimal performance of either class of measurements is notoriously difficult. In fact, instead of finding the optimal measurements, it is easier (and more common) to evaluate bounds on their precision. The most widely-used precision bounds are quantum generalisations of the classical Cramér-Rao bound (CRB) [14, 29–32]. These include the quantum Fisher information (QFI)-based CRBs [14, 29, 30], the Holevo CRB (HCRB) [31], the Nagaoka-Hayashi CRB (NHCRB) [32, 33], and the Gill-Massar CRB (GMCRB) [21]. Whereas the QFI-based CRBs are generally not tight, the HCRB is attainable in the asymptotic limit by performing collective measurements on a large number of states [20, 34–36]. On the

\* Aritra.Das@anu.edu.au

<sup>1</sup> This is in contrast to single-parameter estimation, where entangled measurements over multiple copies of separable states yield no advantage in terms of scaling of variance with number of copies [1].

other hand, the NHCrb bounds the variance for individual measurements and, in many cases, can be proven to be attainable.

Armed with these bounds, we study how far off the collective-optimal precision can be from the individual-optimal one by looking at their ratio. Specifically, by investigating the maximum ratio between the NHCrb and the HCRB, we identify situations where collective quantum measurements are the most advantageous. Our preliminary results show that the ratio of precisions (defined later) is smaller than the number of unknown parameters being estimated,  $n$ . So we focus on state tomography, where the number of parameters is maximal,  $n = n_{\max}$ . For the qubit tomography case, we extrapolate existing results to find a decreasing trend of the ratio with purity [37]. Motivated by this, we propose a model of estimating the coefficients of the generalised Gell-Mann matrices (GMMs) [38], which extend the Pauli matrices to higher dimensions, in mixed  $d$ -dimensional qudit states [39]. This “linear GMM model” is symmetric enough to admit analytical results in the full-parameter case ( $n = n_{\max}$ ). We then extend these results via arguments based on semi-definite programming (SDP) to tomography in any other basis and to the  $n < n_{\max}$  case.

A summary of our main findings on the ratio between the collective- and individual-optimal precisions for local estimation from smooth models on  $d$ -dimensional qudits follows:

- for any model comprising  $n$  parameters, the ratio is at most  $n$  (proved in Sec. III A),
- for tomography of the maximally-mixed state in any basis, the ratio is at most  $d + 1$  (proved to be tight for GMM basis in Sec. IV A, and to be valid for other bases in Appendix G),
- for tomography of any state in any basis, the ratio is at most  $d + 2^2$  (proved for GMM basis in Sec. IV B, numerically shown for other bases in Appendix G),
- for estimating any number of GMM basis coefficients of the maximally-mixed state, the ratio is at most  $d + 1$  (proved in Sec. IV C),
- for tomography in the GMM basis, the maximum ratio at fixed (known) purity is in  $O(d)$  and is at most  $d + 1$  (numerical result in Sec. IV D),
- for any model comprising  $n$  parameters, the ratio is at most  $\min(n, d + 1)$  (conjecture).

The rest of our paper is structured as follows. In Sec. II we provide a brief background on parameter estimation and precision bounds. Then in Sec. III we present some preliminary results and introduce our main model. In

Sec. IV we present our methodology for obtaining the maximum ratio for this model, treating the maximally-mixed state in Subsec. IV A and arbitrary states in Subsec. IV B, whilst deferring mathematical proofs to Appendices A–J. We solve a related model in Sec. IV C and present further numerical results in Sec. IV D, before closing with a brief discussion in Sec. V.

## II. BACKGROUND

In this section, we present a brief recap on quantum parameter estimation, precision bounds and known relationships between them. We also introduce our model of estimating generalised GMMs on parameterised qudit states, along with a summary of results for the  $d = 2$  case of qubit Bloch vector estimation from Ref. [37]

The general recipe to estimate  $n$  parameters  $\theta := \{\theta_j\}_{j \in [n]} \in \Theta$  (where we define  $[n] := \{1, \dots, n\}$  and denote by  $\Theta$  the set of all possible parameter values) of a quantum state  $\rho_\theta$  involves two steps. First, one performs quantum measurements, generally positive operator-valued measures (POVMs)  $\{\Pi_k\}_{k \in [m]}$  with  $m$  outcomes, on  $\rho_\theta$ . Second, a classical estimator operator  $\hat{\theta}_{jk}$  is constructed that assigns an estimated value to  $\theta_j$  for each measurement outcome  $k \in [m]$ , which occurs with probability  $p_k := \text{Tr}(\rho_\theta \Pi_k)$ . Here  $\text{Tr}$  (in serif font) denotes tracing over the quantum system.

The performance of the estimator is quantified via its mean squared error matrix

$$(V_\theta)_{jk} := \sum_{l \in [m]} (\hat{\theta}_{jl} - \theta_j)(\hat{\theta}_{kl} - \theta_k) p_l, \quad (1)$$

the trace of which gives the total average squared deviation  $\text{Tr}(V_\theta) = \sum_{l,j} (\hat{\theta}_{jl} - \theta_j)^2 p_l$ . Here  $\text{Tr}$  (in sans serif font) denotes tracing over the classical or parameter indices. In this work, we focus on local estimation, wherein the parameters of interest are assumed to be close to their true values,  $\theta^* := \{\theta_j^*\}_{j \in [n]}$ , i.e.,  $\theta \approx \theta^*$ . For locally-unbiased (LUB) estimators, which have zero bias at the true parameter values,  $V_\theta$  is equivalent to the covariance matrix of parameter estimates and  $\text{Tr}(V_\theta)$  is simply the total variance.

Precision bounds lower-bound the uncertainties in estimating multiple (possibly) incompatible parameters. In this work, we focus on precision bounds on  $\text{Tr}(V_\theta)$ ; the classical CRB yields a lower bound to this via

$$V_\theta \succcurlyeq J^{-1} \implies \text{Tr}(V_\theta) \geq \text{Tr}(J^{-1}), \quad (2)$$

where  $A \succcurlyeq B$  denotes positive semi-definiteness of  $A - B$ , and  $J \equiv J(\rho_\theta, \{\Pi_j\}_{j \in [m]})$  is the classical Fisher information (CFI) tensor. The CFI (defined later in Eq. (26)) is best understood as a measure on the parameter space  $\Theta \subseteq \mathbb{R}^n$  of the local sensitivity of measurements  $\{\Pi_j\}_{j \in [m]}$  towards each  $\theta_j$  when measuring state  $\rho_\theta$ . Minimising  $\text{Tr}(J^{-1})$  in Eq. (2) over all possible measurements  $\{\Pi_j\}_{j \in [m]}$  yields the so-called most

<sup>2</sup> This bound is loose; we suspect the attainable bound to be  $d + 1$ .

informative CRB [33], representing the ultimate precision attainable via individual measurements,

$$C_{\text{MI}} := \min_{\{\Pi_j\}_{j \in [m]}} \text{Tr}(J^{-1}). \quad (3)$$

A different precision bound on  $\text{Tr}(V_\theta)$  for the separable-measurement case, proposed by Nagaoka [33] and modified by Hayashi [16], is the NHCRB,

$$C_{\text{NHCRB}} := \min_{\mathbb{L}, \mathbb{X}} \left\{ \text{Tr}[\mathbb{S}_\theta \mathbb{L}] \mid \mathbb{L} \succcurlyeq \mathbb{X} \mathbb{X}^\top, \right. \\ \left. \mathbb{L}_{jk} = \mathbb{L}_{kj} \text{ Hermitian} \right\} - \text{Tr}(\theta \theta^\top). \quad (4)$$

Here  $\mathbb{X} := \{X_1, \dots, X_n\}^\top$  are the Hermitian LUB estimators that satisfy (abbreviating  $\frac{\partial}{\partial \theta_j}$  as  $\partial_j$ )

$$\text{Tr}(\rho_\theta X_j) = \theta_j \quad \& \quad \text{Tr}(\partial_j \rho_\theta X_k) = \delta_{jk}, \quad (5)$$

and  $\mathbb{S}_\theta = \mathbb{1}_n \otimes \rho_\theta$ ,  $\text{Tr}$  denotes trace over both classical and quantum subsystems,  $^\top$  denotes transpose with respect to the classical (parameter) index, and blackboard fonts represent classical-quantum matrices.

On the other hand, the HCRB is a collective-measurement precision bound on  $\text{Tr}(V_\theta)$ , defined as

$$C_{\text{HCRB}} := \min_{\mathbb{X}} \left\{ \text{Tr}(\mathbb{Z}_\theta[\mathbb{X}]) + \|\text{Im} \mathbb{Z}_\theta[\mathbb{X}]\|_1 - \text{Tr}(\theta \theta^\top) \right\}, \\ \mathbb{Z}_\theta[\mathbb{X}]_{jk} := \text{Tr}(\rho_\theta X_j X_k), \quad (6)$$

where  $\|X\|_1 := \text{Tr}(\sqrt{X^\dagger X})$  denotes the trace norm. An equivalent expression for  $C_{\text{HCRB}}$ , written in a similar form as Eq. (4), is

$$C_{\text{HCRB}} := \min_{\mathbb{L}, \mathbb{X}} \left\{ \text{Tr}[\mathbb{S}_\theta \mathbb{L}] \mid \text{Tr}[\mathbb{S}_\theta \mathbb{L}] \text{ real \& symmetric}, \right. \\ \left. \text{Tr}[\mathbb{S}_\theta \mathbb{L}] \succcurlyeq \text{Tr}[\mathbb{S}_\theta \mathbb{X} \mathbb{X}^\top] \right\} - \text{Tr}(\theta \theta^\top). \quad (7)$$

Notably, the minimisations in Eqs. (4), (6) and (7) have no explicit closed-form solution for general mixed states  $\rho_\theta$  [40] and are typically evaluated numerically via SDPs [19, 41].

Besides  $C_{\text{HCRB}} \leq C_{\text{NHCRB}}$ , the following ordering between the various precision bounds is known

$$\max(C_{\text{SLD}}, C_{\text{RLD}}) \leq C_{\text{HCRB}} \leq C_{\text{NHCRB}} \leq C_{\text{MI}}. \quad (8)$$

Here  $C_{\text{SLD}}$  and  $C_{\text{RLD}}$  are, respectively, the symmetric logarithmic derivative (SLD) and the right-logarithmic derivative (RLD) CRBs (see Appendix D for definitions). We know that all three inequalities in Eq. (8) are saturated for single-parameter estimation [28]. Moreover,  $C_{\text{NHCRB}} = C_{\text{HCRB}}$  for estimating any number of parameters from pure states [28]. On the other hand, if the single-copy NHCRB and the HCRB are unequal, this gap persists between the finite-copy NHCRB and the HCRB, shrinking asymptotically with the number of copies [42]. Lastly, the HCRB is known to be at most twice the SLD CRB, i.e.,  $C_{\text{SLD}} \leq C_{\text{HCRB}} \leq 2C_{\text{SLD}}$  [43, 44].

Surprisingly, a similar relationship between the HCRB and the NHCRB is not known, leading to a gap in our knowledge of the potential quantum advantage offered by collective measurements. Specifically, in this work, we shall analyse the collective quantum enhancement

$$\mathcal{R}[\{\rho_\theta \mid \theta \in \Theta\}] := \max_{\theta \in \Theta} \frac{C_{\text{NHCRB}}[\rho_\theta]}{C_{\text{HCRB}}[\rho_\theta]}, \quad (9)$$

for a quantum statistical model  $\{\rho_\theta \mid \theta \in \Theta\}$ , where the maximum is over all possible parameter values. This quantity can be interpreted as the maximum quantum enhancement obtainable from using collective measurements over separable measurements for this model. A further maximisation over all full-rank quantum models is possible,

$$\mathcal{R} := \max_{\text{full-rank models}} \mathcal{R}[\{\rho_\theta \mid \theta \in \Theta\}], \quad (10)$$

corresponding to the ultimate collective quantum enhancement in precision [3, 45]. In the following we abbreviate  $\mathcal{R}[\{\rho_\theta \mid \theta \in \Theta\}]$  as  $\mathcal{R}[\rho_\theta]$  while specifying the model explicitly. We are also interested in the case where the maximisation over full-rank models is restricted to either  $d$ -dimensional probe states, or estimating  $n$  parameters, or both, with  $d$  and  $n$  fixed and known.

### III. PRELIMINARIES

In this section, we establish some preliminary results based on recent work and introduce our model. First, in Subsec. III A we establish a problem-independent upper bound of  $n$  on the ultimate collective enhancement  $\mathcal{R}$ . Then, in Subsec. III B, we introduce our model, the linear GMM model, and identify one of its unique features.

#### A. Ratio of $n$

We now establish a model-agnostic (or problem-independent) upper bound of  $n$  on the ultimate collective enhancement  $\mathcal{R}$ , for estimating  $n$  parameters. Using Ref. [46]'s upper bound (based on Ref. [47]) to the NHCRB,

$$C_{\text{NHCRB}} \leq \min_{\mathbb{X}} \left\{ \text{Tr}(\mathbb{Z}_\theta[\mathbb{X}]) \right. \\ \left. + \sum_{j,k \in [n]} \|\rho_\theta[X_j, X_k]\|_1 \right\}, \quad (11)$$

and  $\|\rho_\theta[X_j, X_k]\|_1 \leq 1/2 \text{Tr}[\rho_\theta(X_j^2 + X_k^2)]$ , we get

$$C_{\text{NHCRB}} \leq n \min_{\mathbb{X}} \text{Tr}(\mathbb{Z}_\theta[\mathbb{X}]) = n C_{\text{SLD}}. \quad (12)$$

On the other hand, from Eq. (6), we have  $C_{\text{HCRB}} \leq \min_{\mathbb{X}} \text{Tr}(\mathbb{Z}_\theta[\mathbb{X}])$  so that  $C_{\text{NHCRB}}/C_{\text{HCRB}} \leq n$  and thus

$$\mathcal{R} \leq n. \quad (13)$$

Note that under the assumption of independent parameters  $\theta$ , we have  $n \leq n_{\max}$  [21], so that Eq. (13) implies  $\mathcal{R} \leq n_{\max} = d^2 - 1$ .

### B. Model: Estimating GMMs from Qudits

We now introduce our quantum statistical model, which is an  $n_{\max}$ -parameter family of  $d$ -dimensional qudit states. This model, which we call the ‘linear GMM model’, involves estimating the  $n_{\max}$  coefficients  $\{\theta_j\}_{j \in [n_{\max}]}$  of the GMMs  $\Lambda_d := \{\lambda_j\}_{j \in [n_{\max}]}$  from the Bloch representation of a qudit state [39],

$$\rho_\theta = \mathbb{1}_d/d + \sum_{j=1}^{n_{\max}} \theta_j \lambda_j. \quad (14)$$

The GMMs  $\Lambda_d$  are traceless, Hermitian generalisations of the qubit Pauli operators (see Appendix A), and the decomposition in Eq. (14) is a one-to-one map between the Hilbert space  $\mathcal{H}_d$  of  $\rho_\theta$  and the parameter space  $\Theta \subset \mathbb{R}^{n_{\max}}$ . Estimating  $\theta$  is thus equivalent to qudit state tomography. Note that we adopt the convention of normalising the GMMs such that  $\text{Tr}(\lambda_j \lambda_k) = \delta_{jk}$ <sup>3</sup>.

It is useful to summarise the  $d = 2$  case results here [37]; the HCRB and NHCRB are

$$\begin{aligned} C_{\text{HCRB}} &= C_{\text{RLD}} = 3 - r^2 + 2r, \\ C_{\text{NHCRB}} &= C_{\text{GMCRB}} = 5 - r^2 + 4\sqrt{1 - r^2} \end{aligned} \quad (15)$$

with  $r^2 = \sum_j \theta_j^2 = \text{Tr}(\rho^2) - 1/2$  the squared length of the Bloch vector. In this case, the NHCRB is attained by measuring informationally-complete (IC) POVMs, simplifying to symmetric informationally-complete (SIC) POVMs (see Eq. (25) for definition) at  $r = 0$  [37]. It is straightforward<sup>4</sup> to see from Eq. (15) that the ratio  $C_{\text{NHCRB}}/C_{\text{HCRB}}$  is maximised at  $r = 0$ , corresponding to estimating parameters of the maximally-mixed state. Thus, for the qubit tomography model, the maximum enhancement  $\mathcal{R}[\{\rho_\theta\}]$  is three, and this ratio is attained when estimating the three Pauli matrix coefficients of the maximally-mixed qubit state [37].

An important simplifying feature of the linear GMM model is that the LUB estimators  $\mathbb{X} = \{X_1, \dots, X_n\}^\top$  are uniquely fixed to be the GMMs themselves, i.e.,

$$X_j = \lambda_j. \quad (16)$$

That there is exactly one feasible solution for the LUB estimators<sup>5</sup> significantly simplifies the evaluation of the

bounds. To see this unique feature of our model, consider that the true (unknown) state is

$$\rho_\theta^* = \mathbb{1}_d/d + \sum_{j=1}^{n_{\max}} \theta_j^* \lambda_j.$$

The LUB constraints (Eq. (5)) at  $\theta^*$  are then

$$\text{Tr}(\rho_\theta X_k)|_{\theta=\theta^*} = \theta_k^* \quad \text{and} \quad \text{Tr}(\partial_j \rho_\theta X_k)|_{\theta=\theta^*} = \delta_{jk}. \quad (17)$$

Writing  $X_j = \sum_k c_{jk} \lambda_k$ , where  $c_{jk}$  are unknown real numbers (to preserve Hermiticity of  $X_j$ ), reduces Eq. (17) to

$$\sum_j c_{kj} \theta_j^* = \theta_k^* \quad \& \quad c_{kj} = \delta_{jk},$$

which immediately implies  $X_j = \lambda_j$ , as claimed.

## IV. METHODS & RESULTS

In this section, we present our methodology for characterising the maximum collective enhancement for the linear GMM model. First, we study the tomography of maximally-mixed qudit states in Subsec. IV A and show the enhancement here is exactly  $d + 1$ . Next, in Subsec. IV B, we extend our arguments to arbitrary qudit states, establishing a maximum collective enhancement of  $d + 2$ . In Subsec. IV C, we explore the related model of estimating fewer than  $n_{\max}$  parameters of the maximally-mixed state and show that the maximum enhancement remains  $d + 1$ . Finally, in Subsec. IV D, we present numerical results for the maximum enhancement at fixed probe purity, which we find to be in  $\mathcal{O}(d)$ , and for the maximum enhancement for arbitrary parameterisations of arbitrary qudit states.

### A. Ratio of $d + 1$ : Maximally-mixed State

We now investigate the parameter estimation of  $\theta$  ( $n = n_{\max}$ ) for the maximally-mixed qudit state  $\rho_\theta^* = \mathbb{1}_d/d =: \rho_m$  in  $d$  dimensions (corresponding to  $\theta^* = 0$ ). For  $\rho_m$ , we calculate the SLD and RLD CRBs, the HCRB, the NHCRB, and the GMCRB. We also find the SIC-POVM in  $d$  dimensions to be an optimal individual measurement that attains the NHCRB, thus establishing  $C_{\text{MI}} = C_{\text{NHCRB}}$  for this case [33]. Choosing  $\rho_\theta^* = \rho_m$  simplifies the evaluation of various CRBs as this choice of  $\rho_\theta^*$  commutes with every linear operator.

From their definitions, (see Eqs. (D2) and (D3) in Appendix D), we find both the SLD and the RLD operators to be simply

$$L_j^{\text{SLD}} = L_j^{\text{RLD}} = d \lambda_j. \quad (18)$$

<sup>3</sup> Some authors [48] instead normalise as  $\text{Tr}(\lambda_j \lambda_k) = 2\delta_{jk}$  to be consistent with the  $d = 2$  case for Pauli matrices. Our convention rescales the parameter values and bounds, but leaves their ratios invariant.

<sup>4</sup>  $C_{\text{HCRB}}$  increases with  $r$  whereas  $C_{\text{NHCRB}}$  decreases.

<sup>5</sup> This is not generally true, e.g., in Refs. [19, 23] and Appendix F, where  $X_j = \sum_k c_{jk} \lambda_k$  for  $j \in [n]$  and unknown  $c_{jk} \in \mathbb{R}$ .



The two resulting QFI matrices are equal and diagonal (see Appendix D),

$$J^{(\text{SLD})} = J^{(\text{RLD})} = \begin{bmatrix} d & 0 & \dots & 0 \\ 0 & d & \dots & \vdots \\ \vdots & \vdots & \ddots & 0 \\ 0 & \dots & 0 & d \end{bmatrix}_{n \times n}, \quad (19)$$

which is a sign that our model is “locally classical” [13, 49]. The two QFIs then yield their respective CRBs,

$$C_{\text{SLD}} = C_{\text{RLD}} = \frac{n_{\text{max}}}{d} = \frac{d^2 - 1}{d}. \quad (20)$$

As expected of a locally classical model, the HCRB coincides with the SLD CRB and RLD CRB [13, 49]. In fact, any full parameter model ( $n = n_{\text{max}}$ ) with linearly-independent parameter derivatives constitutes a “D-invariant” model, for which  $C_{\text{HCRB}} = C_{\text{RLD}}$  is known to hold [31, 49]. Nonetheless, and more directly, note that the minimisation over  $\mathbb{X}$  in the definition in Eq. (6) is redundant due to the uniqueness discussed in Sec. III B. Thus,  $(Z_\theta[\mathbb{X}])_{jk} = \frac{1}{d} \text{Tr}(\lambda_j \lambda_k) = \delta_{jk}/d$ , which is exactly  $J^{(\text{SLD})^{-1}}$ . Correspondingly,

$$C_{\text{HCRB}} = \text{Tr}(Z_\theta[\mathbb{X}]) = \text{Tr}(J^{(\text{SLD})^{-1}}) = \frac{d^2 - 1}{d} = C_{\text{SLD}}.$$

We write this result as Lemma 1, and defer the detailed proof to Appendix C. Note that, more generally,  $C_{\text{SLD}} = \min_{\mathbb{X}} \{\text{Tr}(Z_\theta[\mathbb{X}])\}$ , so that when  $\mathbb{X}$  is uniquely fixed,  $C_{\text{HCRB}} \geq C_{\text{SLD}}$  implies

$$C_{\text{HCRB}} \geq \text{Tr}(Z_\theta[\mathbb{X}]) = \text{Tr}(\mathbb{S}_\theta \mathbb{X} \mathbb{X}^\top). \quad (21)$$

**Lemma 1.** *The HCRB for estimating  $\theta \approx 0$  from  $\rho_m$  is*

$$C_{\text{HCRB}} = \frac{d^2 - 1}{d}. \quad (22)$$

The NHCRB is not as trivial to compute because despite  $\mathbb{X}$  being uniquely fixed, there is still a minimisation over  $nd \times nd$  matrix  $\mathbb{L}$  in Eq. (4) [19]. Moreover, directly proving the optimality of a candidate  $\mathbb{L}$  is difficult—for this purpose we turn to the SDP formulation of the NHCRB [19] (see Appendix E for definition). The SDP approach offers a simple way to prove optimality via duality: if we can find a primal-feasible solution and a dual-feasible solution such that the primal objective value equals the dual objective value, then the solutions are optimal. In Appendix E, we present a pair of such solutions and prove their optimality using this approach. The optimal argument  $\mathbb{L}^*$  we find to the SDP is

$$\mathbb{L}_{jk}^* = \left( \frac{d+1}{d+2} \right) (\{\lambda_j, \lambda_k\} + \delta_{jk} \mathbb{1}_d) \quad (23)$$

where  $j, k \in [n]$  and  $\{\cdot, \cdot\}$  denotes the anti-commutator. Directly computing  $\text{Tr}[\mathbb{S}_\theta \mathbb{L}^*]$  then leads to the following lemma.

**Lemma 2.** *The NHCRB for estimating  $\theta_j \approx 0$  from  $\rho_m$  is*

$$C_{\text{NHCRB}} = \frac{(d^2 - 1)(d + 1)}{d}. \quad (24)$$

Our first main result now follows straightforwardly from Lemmas 1 and 2.

**Theorem 1.** *For tomography of the maximally-mixed qudit state  $\rho_m = \mathbb{1}_d/d$ , the collective enhancement  $C_{\text{NHCRB}}/C_{\text{HCRB}} = d + 1$ .*

The HCRB is already known to be asymptotically attainable, so we now prove the attainability or tightness of the NHCRB for our model. Specifically, we show that the NHCRB in Lemma 2 can be attained by measuring any rank-one symmetric informationally-complete (SIC) POVM in  $d$  dimensions (assuming one exists). The SIC POVM is a set of  $d^2$  measurement operators  $\{\Pi_j\}_{j \in [d^2]}$  that form a POVM and are completely symmetric between themselves under the trace inner product,

$$\text{Tr}(\Pi_j \Pi_k) = \frac{1}{d^2(d+1)} \quad \forall j \neq k. \quad (25)$$

To prove that measuring SIC POVMs attains the NHCRB, we show that the measured probabilities  $\text{Tr}(\rho_m \Pi_j)$  directly yield a variance equal to  $C_{\text{NHCRB}}$  from Lemma 2, establishing  $C_{\text{MI}} = C_{\text{NHCRB}}$  in this case. The CFI matrix  $J_{jk}$  ( $j, k \in [n]$ ), which in the multi-parameter case is given by

$$J_{jk}[\{\Pi_l\}_{l \in [m]}] = \sum_{l=1}^m \frac{\text{Tr}[\partial_j \rho_\theta \Pi_l] \text{Tr}[\partial_k \rho_\theta \Pi_l]}{\text{Tr}[\rho_\theta \Pi_l]}, \quad (26)$$

simplifies to (see Lemma 7 and proof in Appendix E 5)

$$J_{jk} = d^2 \sum_{m=1}^{d^2} \text{Tr}[\lambda_j \Pi_m] \text{Tr}[\lambda_k \Pi_m] = \delta_{jk} \frac{d}{d+1} \quad (27)$$

in this case, so that Eq. (2) then leads to

$$\text{Tr}(J^{-1}) = \frac{(d^2 - 1)(d + 1)}{d} = C_{\text{NHCRB}}. \quad (28)$$

From Eq. (3), we then have  $C_{\text{MI}} \leq \text{Tr}(J^{-1}) = C_{\text{NHCRB}} \leq C_{\text{MI}}$  with the last inequality from Eq. (8). This proves  $C_{\text{MI}} = C_{\text{NHCRB}}$ , meaning that the ultimate individual precision is attained for this model by measuring SIC POVMs. Notably, any rank-one SIC POVM in  $d$  dimensions, irrespective of its orientation, constitutes an optimal individual measurement in this scenario. An alternative proof of this attainability can be furnished using the Gill-Massar Cramér-Rao bound (GMCRA) [21], which also applies to the individual measurement setting (see Appendix H).

### B. Ratio of $d + 2$ : Extension to Arbitrary States

In this section, we extend Lemmas 1 & 2 and Theorem 1 for  $\rho_m$  to arbitrary qudit states  $\rho_\theta \neq \rho_m$ . Such a qudit state can still be written as in Eq. (14), but now the true parameter values  $\theta^*$  are non-zero and  $\theta \approx \theta^*$ . In this case, we show that  $C_{\text{HCRB}}[\rho_\theta] \geq C_{\text{HCRB}}[\rho_m] - \sum_{j \in [n]} \theta_j^{*2}$  and that  $C_{\text{NHCRB}}[\rho_\theta] \leq C_{\text{NHCRB}}[\rho_m] - \sum_{j \in [n]} \theta_j^{*2}$ , which, we then show, imply

$$\frac{C_{\text{NHCRB}}[\rho_\theta]}{C_{\text{HCRB}}[\rho_\theta]} \leq d + 2.$$

This establishes the maximum collective quantum enhancement  $\mathcal{R}[\{\rho_\theta\}]$  for the linear GMM model to be  $d + 2$ . We also argue that the optimal individual measurements are now IC POVMs, supported by numerical results in Appendix I.

The HCRB and the NHCRB involve an additional  $-\text{Tr}(\theta^* \theta^{*\top}) = -\sum_{j \in [n]} \theta_j^{*2}$  term for non-zero  $\theta^*$  (Eqs. (4), (6) & (7)). For the HCRB, it is simple to see from Eq. C6 in Appendix C that  $\text{Tr}(\mathbb{S}_\theta \mathbb{X} \mathbb{X}^\top)$  still lower-bounds  $\min_{\mathbb{L}, \mathbb{X}} \text{Tr}(\mathbb{S}_\theta \mathbb{L})$  (see also Remark 1 in Appendix C) so that

$$C_{\text{HCRB}}[\rho_\theta] \geq \text{Tr}(\mathbb{S}_\theta \mathbb{X} \mathbb{X}^\top) - \sum_{j \in [n]} \theta_j^{*2} \quad (29)$$

despite  $\mathbb{L} = \mathbb{X} \mathbb{X}^\top$  not being the optimal solution anymore. Note also that the purity of the true state  $\rho_\theta^*$  is

$$P(\rho_\theta^*) = \text{Tr}((\rho_\theta^*)^2) = 1/d + \sum_{j \in [n]} \theta_j^{*2}.$$

By explicit calculation, we find  $\text{Tr}(\mathbb{S}_\theta \mathbb{X} \mathbb{X}^\top) = d^2 - 1/d = C_{\text{HCRB}}[\rho_m]$ , and hence,

$$C_{\text{HCRB}}[\rho_\theta] \geq \frac{d^2 - 1}{d} - \sum_{j \in [n]} \theta_j^{*2} = d - P(\rho_\theta^*). \quad (30)$$

From Lemma 1, we know that this inequality is saturated by the maximally-mixed state  $\rho_m$ , which has purity  $1/d$ . Fig. 1 (a) depicts how  $d - P(\rho_\theta^*)$  compares with the actual HCRB for qutrit states.

For the NHCRB, our key insight is that the optimal argument  $\mathbb{L}_{jk}^* = d^{-1/d+2} (\{\lambda_j, \lambda_k\} + \delta_{jk} \mathbb{1}_d)$  from Lemma 3 in Sec. IV A is still feasible:  $\mathbb{L}^*$  satisfies the constraints  $\mathbb{L}_{jk} = \mathbb{L}_{kj}$  Hermitian and  $\mathbb{L} \succcurlyeq \mathbb{X} \mathbb{X}^\top$ , which are all independent of  $\rho_\theta$ . However,  $\mathbb{L}^*$  is not optimal so  $\text{Tr}[\mathbb{S}_\theta \mathbb{L}^*]$  only upper-bounds  $\min_{\mathbb{L}} \text{Tr}[\mathbb{S}_\theta \mathbb{L}]$  in Eq. (4). Again, we explicitly calculate  $\text{Tr}[\mathbb{S}_\theta \mathbb{L}^*]$  to find

$$\text{Tr}[\mathbb{S}_\theta \mathbb{L}^*] = \frac{(d^2 - 1)(d + 1)}{d} = C_{\text{NHCRB}}[\rho_m]$$

so that we can upper-bound the NHCRB as

$$\begin{aligned} C_{\text{NHCRB}}[\rho_\theta] &\leq \frac{(d^2 - 1)(d + 1)}{d} - \sum_j \theta_j^{*2} \\ &= d^2 + d - 1 - P(\rho_\theta^*). \end{aligned} \quad (31)$$

From Lemma 2, we see that the inequality in Eq. (31) is saturated by the maximally-mixed state  $\rho_m$ . Fig. 1 (b) depicts how  $d^2 + d - 1 - P(\rho_\theta^*)$  compares with the actual NHCRB for qutrit states.

**Theorem 2.** *For tomography on arbitrary  $d$ -dimensional qudit state  $\rho_\theta$ , the maximum collective enhancement  $\mathcal{R}[\{\rho_\theta\}] = \max_{\theta \in \Theta} C_{\text{NHCRB}}[\rho_\theta] / C_{\text{HCRB}}[\rho_\theta] \leq d + 2$ .*

*Proof.* Combining the lower bound for the HCRB in Eq. (30) with the upper bound for the NHCRB in Eq. (31), we get

$$\frac{C_{\text{NHCRB}}[\rho_\theta]}{C_{\text{HCRB}}[\rho_\theta]} \leq \frac{d^2 + d - 1 - P(\rho_\theta)}{d - P(\rho_\theta)}. \quad (32)$$

Then, using  $1/d \leq P(\rho_\theta) \leq 1$ , we find the maximum of the right hand side of Eq. (32) to be  $d + 2$ , attained when  $P(\rho_\theta) = 1$ , i.e., when  $\rho_\theta$  is pure.  $\square$

Theorem 2 establishes a loose upper bound that we expect to never be attained. The ratio between the two bounds is actually maximised by maximally-mixed states and minimised by pure states. This discrepancy is due to the HCRB lower bound in Eq. (29) being a decreasing function of purity, whereas numerical results (Sec. IV D and Appendix G) and the qubit case (Eq. (15)) show the HCRB to be an increasing function of purity for this model. And using  $C_{\text{HCRB}}[\rho_\theta] \geq C_{\text{HCRB}}[\rho_m]$  instead of Eq. (29) in the proof of Theorem 2 leads to an upper bound of  $d + 1$  on the ratio; this is a tight bound and is saturated by the model considered in Sec. IV A. Nonetheless, Theorems 1 and 2 together establish that for the linear GMM model,  $\mathcal{R}[\{\rho_\theta\}] \leq d + 2$ .

We extend the upper bounds on the ratio proved in Secs. IV A and IV B to arbitrary, full-rank, parameter-independent weight matrices  $W$  in Appendix G. Arbitrary weight matrices correspond to reparameterisations of the model [13, 19, 50], i.e., estimating parameters that are not coefficients of the GMMs. Our results in Appendix G prove that for the maximally-mixed state  $\rho_m$ , and for estimating any  $n_{\text{max}}$  independent parameters locally, the maximum collective enhancement is at most  $d + 1$ . We also numerically show that when estimating from any other state  $\rho_\theta$ , the ratio is smaller than when estimating from  $\rho_m$  with the same weight  $W$ . This suggests the maximum quantum enhancement from collective measurements over individual measurements in any local tomography problem is  $d + 1$ , i.e.,

$$\max_{\substack{\text{full-rank,} \\ \text{full-parameter} \\ \text{models}}} \mathcal{R}[\{\rho_\theta\}] \leq d + 1, \quad (33)$$

and this upper bound is attained by the model studied in Sec. IV A.

Finally, the optimal separable measurements, assuming all the  $\theta_j$  to be independent, are IC-POVMs. This is because to estimate  $d^2 - 1$  independent parameters, one needs  $d^2 - 1$  independent probabilities which can only

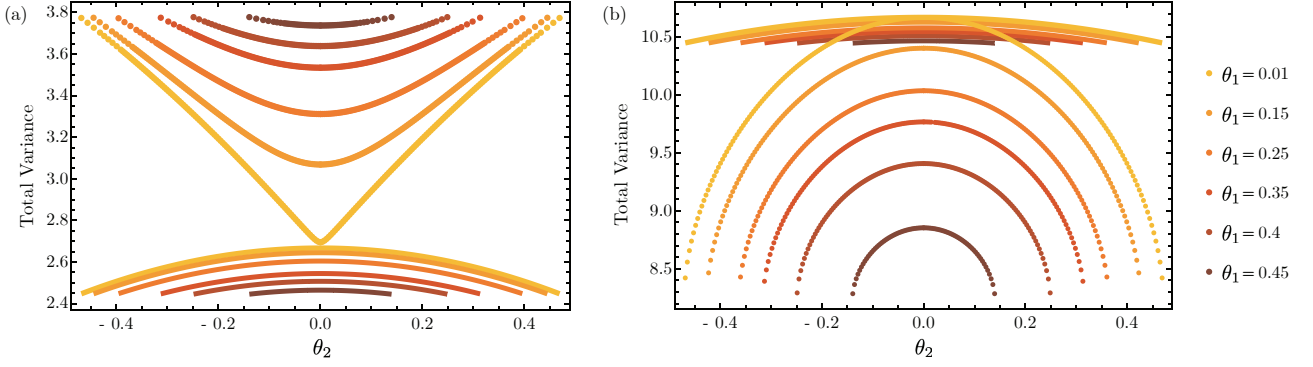


FIG. 1. Comparison of the HCRB and the NHCRB to their lower and upper bounds, respectively. (a) HCRB and its lower bound  $d - P(\rho_\theta)$  (from Eq. (30)). The lower solid parabolic curves show the lower bound and the upper triangular curves (beginning and ending with dots) show the numerically-computed HCRB. (b) NHCRB and its upper bound  $d^2 + d - 1 - P(\rho_\theta)$  (from Eq. (31)). The lower dotted curves show the numerically-computed NHCRB and the upper solid curves show the upper bound. The state chosen in both (a) and (b) is a mixed qutrit  $\rho_\theta = \mathbb{1}_d/d + \theta_1\lambda_2 + \theta_2\lambda_4$ .

arise from measuring a POVM with at least  $d^2$  linearly independent elements. Having any more than  $d^2$  POVM elements is also redundant, as the extra elements cannot be linearly independent from the first  $d^2$  elements. In Appendix I, we depict the transition from SIC POVMs to IC POVMs as the purity of  $\rho_\theta$  increases from  $1/d$  for the maximally-mixed state to 1 for pure states. This result is in line with previous findings that IC POVMs are optimal for state estimation and tomography [51, 52].

### C. Related Model: Estimating $n < n_{\max}$ GMMs

In Secs. IV A and IV B, we studied the full-parameter linear GMM model for the cases  $\theta^* = 0$  and  $\theta^* \neq 0$ . In this section, we study the GMM model with  $n < n_{\max}$  parameters, with the remaining  $n_{\max} - n$  parameters set to zero, i.e., estimating  $\{\theta_j\}_{j \in [n]} \in \Theta$  from

$$\rho_\theta = \mathbb{1}_d/d + \sum_{j \in [n]} \theta_j \lambda_j. \quad (34)$$

The case with  $\{\theta_j\}_{j \in [n_{\max}] \setminus [n]} \neq 0$  is also interesting but we do not study that here. Moreover, we only provide analytic results for the true state  $\rho_\theta^* = \rho_m$ . This is because, numerically, we see that when the parameters not estimated are set to zero, the ratio is maximised by  $\rho_m$ . Although we have not specified which  $n$  GMMs we choose to estimate, and despite the NHCRB (but not the HCRB) depending on this choice,<sup>6</sup> the bounds we provide on the ratio are independent of this choice.

The differentiating factor for this model is that  $X_j = \lambda_j$  are not the sole possible LUB estimators. Nonetheless, for the HCRB, this choice is still optimal, and the HCRB is  $n/d$ , the same form as Lemma 1. For the

NHCRB, we find that linearly modifying  $\Lambda_d$  and bilinearly modifying  $\mathbb{L}_{jk}^*$  from Lemma 3 gives us an upper bound of  $(d+1)n/d$ , also the same form as Lemma 2.

For the HCRB, we again resort to the inequality (Eq. (21))  $C_{\text{HCRB}} \geq \text{Tr}[\mathbb{S}_\theta \mathbb{X} \mathbb{X}^\top]$ , but with the extra observation that for estimating from  $\rho_m$ ,  $\text{Tr}[\mathbb{S}_\theta \mathbb{X} \mathbb{X}^\top]$  is minimised when  $X_j = \lambda_j$  (see Appendix F). Moreover, for  $X_j = \lambda_j$ ,  $\mathbb{L} = \mathbb{X} \mathbb{X}^\top$  satisfies all the constraints and yields

$$\text{Tr}[\mathbb{S}_\theta \mathbb{L}] = \text{Tr}[\mathbb{S}_\theta \mathbb{X} \mathbb{X}^\top] = \frac{n}{d},$$

so that  $C_{\text{HCRB}} = C_{\text{SLD}} = n/d$ , as claimed.

For the NHCRB, the  $X_j$  are linear combinations of the  $d^2 - 1$  GMMs, and, so, can be written as

$$\mathbb{X} = \mathbb{C}^{(2)} \Lambda_d, \quad (35)$$

where  $\mathbb{C}^{(2)}$  is a real matrix. Then,  $\mathbb{X} \mathbb{X}^\top = \mathbb{C}^{(2)} \Lambda \Lambda^\top \mathbb{C}^{(2)\top}$ . We similarly modify  $\mathbb{L}^*$  from Eq. (23) to define  $\mathbb{L}^{**} := \mathbb{C}^{(2)} \mathbb{L}^* \mathbb{C}^{(2)\top}$ , which ensures  $\mathbb{L}^{**} \succcurlyeq \mathbb{X} \mathbb{X}^\top$  because of  $\mathbb{L}^* \succcurlyeq \Lambda \Lambda^\top$  from Lemma 3 in Appendix E. The NHCRB in Eq. (4) then becomes a minimisation over  $\mathbb{L}$  and  $\mathbb{C}^{(2)}$ . However, if we choose our ansatz  $\mathbb{L}^{**}$  for  $\mathbb{L}$  and minimise only over  $\mathbb{C}^{(2)}$ , we should get a larger value, i.e.,

$$\begin{aligned} C_{\text{NHCRB}} &= \min_{\mathbb{L}, \mathbb{C}^{(2)}} \left\{ \text{Tr}[\mathbb{S}_\theta \mathbb{L}] \mid \mathbb{L}_{jk} = \mathbb{L}_{kj} \text{ Hermitian}, \right. \\ &\quad \left. \mathbb{L} \succcurlyeq \mathbb{C}^{(2)} \Lambda \Lambda^\top \mathbb{C}^{(2)\top} \right\} \\ &\leq \min_{\mathbb{C}^{(2)}} \left\{ \text{Tr}[\mathbb{S}_\theta \mathbb{L}^{**}] \mid \mathbb{L}^{**} = \mathbb{C}^{(2)} \Lambda \Lambda^\top \mathbb{C}^{(2)\top} \right\} \\ &= \frac{(d+1)n}{d}. \end{aligned} \quad (36)$$

The inequality in Eq. (36) holds because the second minimisation is performed over a subset of the set over which the first minimisation is performed and the last equality follows after some algebra (see Appendix F). Combining

<sup>6</sup> See Table I in Appendix F

this upper bound on the NHCRB with  $C_{\text{HCRB}} = n/d$ , we get the following theorem.

**Theorem 3.** *For estimating fewer-than- $n_{\text{max}}$  coefficients of GMMs of the maximally-mixed qudit state, the collective enhancement  $C_{\text{NHCRB}}/C_{\text{HCRB}} \leq d + 1$ .*

Numerically, we see this ratio actually depends on  $n$ : as  $n$  increases from 2 to  $d^2 - 1$ , the ratio increases from 2 to  $d + 1$ . Table I in Appendix F depicts this increase by listing the two bounds and their ratios for  $d = 3$ . As proven here, the HCRB only depends on  $n$  and  $d$ . Interestingly, when the true values of the parameters not being estimated are non-zero, the maximally-mixed state is no longer the ratio-maximising state. However, the  $n$  bound in Sec. III A and numerical results in Sec. IV D suggest that the maximum ratio increases with  $n$  at fixed  $d$ . And we have analysed the  $n = n_{\text{max}}$  case in depth, so we expect that for any  $n < n_{\text{max}}$  model, the same bound of  $d + 1$  should hold.

#### D. Numerical Results

Our results from numerical simulations both validate and complement our analytical results. Fig. 1 (a) and (b) show our numerical results for  $d = 3$  and  $\rho_\theta$  close to  $\rho_m$ , i.e., highly mixed qutrit states. It is evident that the lower and upper bounds from Eqs. (30) and (31), respectively, are valid for all  $\rho_\theta$  but saturated only for  $\rho_m$ . In fact, in Fig. 1 (a), our HCRB lower bound is a decreasing function of purity whereas the HCRB is an increasing function of purity. It then follows that  $C_{\text{HCRB}}[\rho_\theta] \geq C_{\text{HCRB}}[\rho_m]$  must hold true, which would imply a maximum collective enhancement of  $d + 1$  instead of  $d + 2$  in Theorem 2.

Directly maximising the ratio  $C_{\text{NHCRB}}/C_{\text{HCRB}}$  over state space  $\mathcal{H}_d$  is computationally demanding for large  $d$ , so we perform repeated-random sampling over  $\mathcal{H}_d$  to study the dependence between maximum ratio and state properties. For each randomly-generated problem instance, we solve the NHCRB and HCRB SDPs numerically and compute their ratio [19]. Further details of the random-sampling procedure used for subsequent results are presented in Appendix J.

In Fig. 2, we plot our random-sampling results for the ratio versus purity in the linear GMM model for  $d = 2, 3$  and 4. For each  $d$ , the overall maximum ratio observed is  $d + 1$ . Interestingly, whereas for qubits the ratio is uniquely determined by purity, the higher dimensionality of the qudit state space allows for a range of ratios at any given purity. We find that the ratio at a given purity is maximised by full-rank depolarised pure states,  $p|\phi\rangle\langle\phi| + (1 - p)\mathbb{1}_d/d$  for any pure state  $|\phi\rangle$  and  $p \in [0, 1]$ . To simplify computation, we choose the more specific family  $\rho_{\text{max}}(p) = p|+\rangle\langle+|_d + (1 - p)\mathbb{1}_d/d$ , where  $|+\rangle_d = (|0\rangle + \dots + |d - 1\rangle)/\sqrt{d}$  and calculate the HCRB to be

$$C_{\text{HCRB}}[\rho_{\text{max}}(p)] = \frac{d^2 - 1}{d} + p(d - 1) - \frac{d - 1}{d}p^2. \quad (37)$$

For the NHCRB, based on numerical evidence for  $d = 3$  to 8, the analytic solutions at the boundary cases  $((d^2 - 1)(d + 1)/d$  at  $p = 0$  and  $2(d - 1)$  at  $p = 1$ ), and the analytic solution for  $d = 2$  (Eq. (15)), we find that

$$C_{\text{NHCRB}}[\rho_{\text{max}}(p)] = \frac{d^2 + 1}{2} - \frac{d^2 - 4d + 5}{2}p^2 + \frac{d^3 + 2d^2 - 3d - 2}{2d}\sqrt{1 - p^2}. \quad (38)$$

Accordingly, the maximum collective enhancement at a fixed purity  $P^*$  is  $C_{\text{NHCRB}}[\rho_{\text{max}}(p^*)]/C_{\text{HCRB}}[\rho_{\text{max}}(p^*)]$  with  $p^* = \sqrt{\frac{P^*d - 1}{d - 1}}$ . Eqs. (37) and (38) reveal that the HCRB grows at most linearly with  $d$ , whereas the NHCRB grows at most quadratically, so that the maximum enhancement at fixed purity (dark red line in Fig. 2) grows at most linearly with dimension and is at most  $d + 1$ .

In contrast to the maximum ratio, the minimum-ratio states (blue dots in Fig. 2) are rank-deficient states<sup>7</sup> of the form  $\rho_{\text{min}}^{(2)}(p) = p|0\rangle\langle 0| + (1 - p)|1\rangle\langle 1|$  for purity greater than  $1/2$ ,  $\rho_{\text{min}}^{(3)}(p) = p|0\rangle\langle 0| + p|1\rangle\langle 1| + (1 - 2p)|2\rangle\langle 2|$  for purity between  $1/3$  and  $1/2$ , and so on<sup>8</sup> down to  $\rho_{\text{min}}^{(d)}$  for purity between  $1/d$  and  $1/(d - 1)$ . This change in form of the minimum-ratio state reflects as the points of non-differentiability in the minimum-ratio curve in Fig. 2.

Whereas all our analytical results are for the linear GMM model, we now provide numerical results for arbitrary smooth models of full-rank qudit states. Specifically, we estimate  $n$  arbitrary independent parameters from arbitrary full-rank  $d$ -dimensional qudit states. In this case, the parameter derivatives  $\partial_j \rho_\theta$  are arbitrary traceless Hermitian operators. Our results for this model are shown in Fig. 3 (and Fig. 9 in Appendix J). Fig. 3 clearly depicts the increase in maximum ratio with number of parameters, in agreement with Secs. III A and IV C. On the other hand, the maximum ratio for a given number of parameters seems to decrease with increasing dimension, but the trend is not perfect due to the relatively small number of samples ( $10^4$ ) for higher dimensions.

#### V. DISCUSSION & CONCLUSION

In this work, we established that for estimating any  $n$  independent parameters, the maximum precision-enhancement from collective measurements can, in principle, be  $n$ . However, at the maximum value of  $n$ , we proved this maximum enhancement to be only  $O(d)$

<sup>7</sup> Although we have treated only full-rank states until now, rank-deficient states can be approximated arbitrarily well by full-rank ones [39].

<sup>8</sup> We only provide analytic expressions for  $\rho_{\text{min}}^{(2)}$  and  $\rho_{\text{min}}^{(3)}$ .



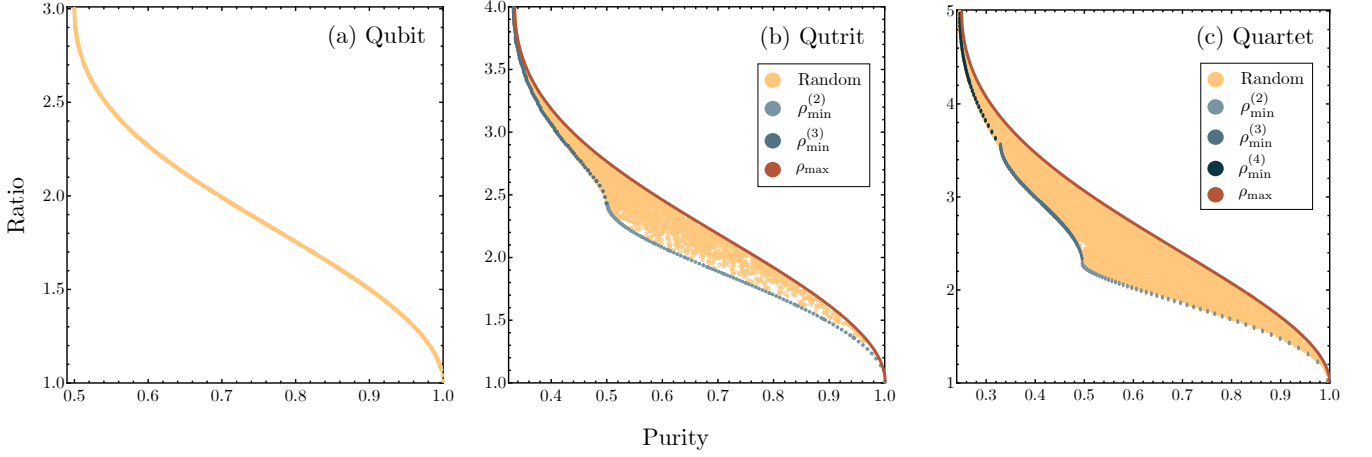


FIG. 2. Ratio between the two bounds versus purity for estimating all  $d^2 - 1$  GMMs from arbitrary states. For qubits (a), over 10,000 samples, we find a one-to-one dependence between ratio and purity. However, for qutrits (b) and quartets (c), over 15,000 and 25,000 samples, respectively, there is a region of allowed ratios at any given purity. The ratio at any purity is maximised by the state  $\rho_{\max}$  and minimised by the states  $\rho_{\min}^{(2)}, \rho_{\min}^{(3)}$  (and  $\rho_{\min}^{(4)}$  in (c)).

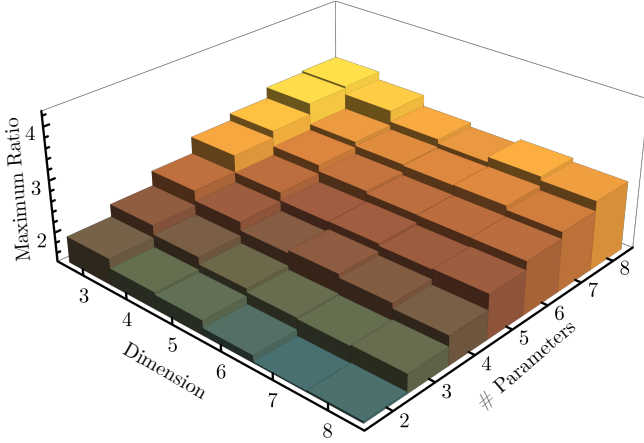


FIG. 3. Random-sampling maximum (10,000 samples each) of ratio for dimensions  $d$  from three to eight and number of parameters  $n$  from two to eight. See Fig. 9 in Appendix J for the distribution of ratios for each  $d$  and  $n$ .

or  $O(\sqrt{n_{\max}})$ . Specifically, for the model of qudit tomography in the Gell-Mann basis, we proved the maximum collective quantum enhancement to be  $d + 2$ , revealing the SIC POVM to be an individual-optimal measurement for the maximally-mixed case. Based on the specific examples provided and our numerical results, we expect the attainable maximum enhancement to be  $d + 1$  instead. We also established a maximum enhancement of  $d + 1$  for tomography in any other basis, i.e., for estimating any other  $d^2 - 1$  parameters. Even when estimating fewer than this maximum number of parameters from the maximally-mixed state, we showed that the upper bound of  $d + 1$  holds. Finally, we numerically demonstrated a maximum enhancement in  $O(d)$  for states of a fixed known purity. Our work thus supple-

ments the known ratio result  $C_{\text{SLD}} \leq C_{\text{HCRB}} \leq 2C_{\text{SLD}}$  with  $C_{\text{SLD}} \leq C_{\text{HCRB}} \leq C_{\text{NHCRB}} \leq (d + 1)C_{\text{HCRB}}$ . Throughout, we have demonstrated our analytical findings via numerics and figures for specific  $d$ .

Our choice of the Gell-Mann basis for tomography was motivated by its symmetry and simplicity, apart from being a generalisation of Pauli matrices. The orthonormality of this basis leads to (local) parameter orthogonality of the basis coefficients [53] for estimating the maximally-mixed state, meaning the Fisher information matrices (both QFIM and CFIM) are diagonal. In this case, the SLD and RLD CRBs equal the HCRB, which are signatures of a D-invariant and locally-classical model [13, 49].

However, the significance of considering the Gell-Mann basis cannot be overstated. Generally, any parameter estimation problem may be linearised about the true parameter values as  $\rho_{\theta} \approx \rho_{\theta^*} + \sum (\theta_j - \theta_j^*) \partial_j \rho_{\theta^*}$ , with the partial derivatives  $\partial_j \rho_{\theta}$  necessarily traceless and Hermitian, meaning they are combinations of GMMs (Sec. VC in [21]). This estimation problem can then be linearly transformed to the equivalent problem of estimating some number of GMM coefficients [13], precisely the model solved in Sec. IV C. For example, the simple result of  $C_{\text{HCRB}}[\rho_m] = n/d$  from Sec. IV A can be directly linearly transformed to obtain a closed-form expression for the HCRB for estimating any  $d^2 - 1$  independent parameters from any full-rank qudit state. Lastly, though our analysis of bounds was specific to tomography in the GMM basis, numerical checks suggest that the bounds and their ratio are invariant for tomography in any other orthonormal basis for the same (traceless and Hermitian) space.

Our approach in this work was to study the quantity  $\mathcal{R}$  by operating at the extreme value of  $n$  for fixed  $d$ , which is  $d^2 - 1$ . A complementary result on the impact of dimensionality on precision and incompatibility in the

multi-parameter setting was recently reported [54]. By defining the normalised gap  $\Delta = (C_{\text{HCRB}} - C_{\text{SLD}})/C_{\text{SLD}}$  ( $0 \leq \Delta \leq 1$ ), the authors studied the asymptotic incompatibility in estimating  $n = 2$  and 3 parameters encoded unitarily onto  $d$ -dimensional qudits. Their results indicate that at fixed  $n$ , increasing  $d$  leads to decreasing asymptotic incompatibility, and that for  $d > n$ , the incompatibility can vanish altogether [54]. A similar effect is seen in our Fig. 3, where, at fixed  $n$ , increasing  $d$  leads to the maximum ratio decreasing. In fact, we can define a finite incompatibility  $\delta = (C_{\text{NHCRB}} - C_{\text{HCRB}})/C_{\text{HCRB}} \leq \mathcal{R} - 1$  based on our results; we have then shown that  $\delta$  can be as large as  $d$ , a significant difference from the asymptotic case.

The results in Fig. 3 and Sec. III A indicate the maximum collective enhancement increases with number of parameters, and hence is highest for state tomography. Moreover, for tomography, the maximum enhancement decreases with purity (Fig. 2) and is maximised by minimum-purity states. Based on this, we conjecture that maximum ratio  $\mathcal{R}$  is attained for tomography of the maximally-mixed state. This case was studied analytically to find a ratio of  $d + 1$ . Hence, we conjecture that  $C_{\text{NHCRB}} \leq (d + 1)C_{\text{HCRB}}$  for all smooth full-rank models in the local estimation setting, i.e.,  $\mathcal{R} = d + 1$ . Notably, both the  $n$  bound (Sec. III A) and the  $d + 1$  bound (Sec. IV) can be tight, with the qubit case (Eq. (15)) being an example of the former. Resultantly, if our conjecture holds true, we would have the stronger condition  $\mathcal{R} = \min(n, d + 1)$ .

In conclusion, we find that for local estimation problems involving  $n$  parameters, the optimal collective measurements are at most  $n$  times more precise than the optimal individual measurements. Although this suggests a collective quantum enhancement of  $n$  is possible, and

that the utility of collective measurements scales with the number of estimated parameters, our further analysis indicates otherwise. By taking the probe dimension  $d$  into account, we upper-bound the collective enhancement by  $d + 1$ , which is a tighter bound for large  $n$  ( $n > d$ ). Our investigation into the utility of collective measurements thus reveals a diminishing payoff in the asymptotic limit. Whereas collective measurements on two copies, three copies, and so on, are practically feasible and outperform the optimal individual measurements, the optimal collective measurements that saturate the HCRB require entangling measurements on asymptotically-large number of copies but only enhance precision by a factor at most linear in dimension, underscoring their non-utility.

Our results apply to multi-parameter quantum metrology and quantum sensing, where a judicious choice between measurement strategies would be resource-wise beneficial. Conversely, our work questions the choice of the HCRB when benchmarking the performance of real-world quantum measurements, and suggests the (finite-copy) NHCRB as a more suitable alternative. Investigating the advantage offered by finite-copy collective measurements, or extending to Bayesian settings could offer valuable insights into the potential of entangling measurements.

## VI. ACKNOWLEDGEMENTS

This research was funded by the Australian Research Council Centre of Excellence CE170100012. This research was also supported by A\*STAR C230917010, Emerging Technology and A\*STAR C230917004, Quantum Sensing. We are grateful to the National Computational Infrastructure (NCI) for their super-computing resources that we used for numerical investigations.

- 
- [1] V. Giovannetti, S. Lloyd, and L. Maccone, Quantum metrology, *Phys. Rev. Lett.* **96**, 010401 (2006).
  - [2] V. Giovannetti, S. Lloyd, and L. Maccone, Advances in quantum metrology, *Nat. Photonics* **5**, 222–229 (2011).
  - [3] M. Szczykulska, T. Baumgratz, and A. Datta, Multi-parameter quantum metrology, *Adv. Phys.: X* **1**, 621–639 (2016).
  - [4] C. M. Caves, Quantum-mechanical noise in an interferometer, *Phys. Rev. D* **23**, 1693 (1981).
  - [5] V. Giovannetti, S. Lloyd, and L. Maccone, Quantum-enhanced positioning and clock synchronization, *Nature* **412**, 417–419 (2001).
  - [6] U. Dorner, R. Demkowicz-Dobrzanski, B. J. Smith, J. S. Lundeen, W. Wasilewski, K. Banaszek, and I. A. Walmsley, Optimal quantum phase estimation, *Phys. Rev. Lett.* **102**, 040403 (2009).
  - [7] M. Kacprowicz, R. Demkowicz-Dobrzański, W. Wasilewski, K. Banaszek, and I. A. Walmsley, Experimental quantum-enhanced estimation of a lossy phase shift, *Nat. Photonics* **4**, 357–360 (2010).
  - [8] H. Yonezawa, D. Nakane, T. A. Wheatley, K. Iwasawa, S. Takeda, H. Arao, K. Ohki, K. Tsumura, D. W. Berry, T. C. Ralph, H. M. Wiseman, E. H. Huntington, and A. Furusawa, Quantum-enhanced optical-phase tracking, *Science* **337**, 1514–1517 (2012).
  - [9] M. Tsang, R. Nair, and X.-M. Lu, Quantum theory of superresolution for two incoherent optical point sources, *Phys. Rev. X* **6**, 031033 (2016).
  - [10] M. Paris and J. Rehacek, *Quantum State Estimation*, Lect. Notes Phys. (Springer Berlin Heidelberg, 2004).
  - [11] M. Hayashi, *Asymptotic Theory of Quantum Statistical Inference: Selected Papers* (World Scientific, 2005).
  - [12] M. G. A. Paris, Quantum estimation for quantum technology, *Int. J. Quantum Inf.* **07**, 125–137 (2009).
  - [13] F. Albarelli, M. Barbieri, M. Genoni, and I. Gianani, A perspective on multiparameter quantum metrology: From theoretical tools to applications in quantum imaging, *Phys. Lett. A* **384**, 126311 (2020).
  - [14] H. Yuen and M. Lax, Multiple-parameter quantum estimation and measurement of nonselfadjoint observables,

- IEEE Trans. Inf. Theory **19**, 740 (1973).
- [15] C. Helstrom and R. Kennedy, Noncommuting observables in quantum detection and estimation theory, *IEEE Trans. Inf. Theory* **20**, 16–24 (1974).
  - [16] M. Hayashi, On simultaneous measurement of noncommutative physical values, in *Development of infinite-dimensional noncommutative analysis*, 1099 (RIMS Kokyuroku, Kyoto Univ., 1999) pp. 96–188.
  - [17] J. S. Sidhu, Y. Ouyang, E. T. Campbell, and P. Kok, Tight bounds on the simultaneous estimation of incompatible parameters, *Phys. Rev. X* **11**, 011028 (2021).
  - [18] C. W. Helstrom, Quantum detection and estimation theory, *J. Stat. Phys.* **1**, 231–252 (1969).
  - [19] L. O. Conlon, J. Suzuki, P. K. Lam, and S. M. Assad, Efficient computation of the Nagaoka–Hayashi bound for multiparameter estimation with separable measurements, *Npj Quantum Inf.* **7**, 110 (2021).
  - [20] S. Massar and S. Popescu, Optimal extraction of information from finite quantum ensembles, *Phys. Rev. Lett.* **74**, 1259 (1995).
  - [21] R. D. Gill and S. Massar, State estimation for large ensembles, *Phys. Rev. A* **61**, 042312 (2000).
  - [22] A. Mansouri, R. A. Abrahao, and J. S. Lundeen, Efficient quantum state tomography using collective measurements, in *Frontiers in Optics + Laser Science 2022 (FIO, LS)* (Optica Publishing Group, 2022) p. FM3B.5.
  - [23] L. O. Conlon, T. Vogl, C. D. Marciniak, I. Pogorelov, S. K. Yung, F. Eilenberger, D. W. Berry, F. S. Santana, R. Blatt, T. Monz, P. K. Lam, and S. M. Assad, Approaching optimal entangling collective measurements on quantum computing platforms, *Nat. Phys.* **19**, 351–357 (2023).
  - [24] M. A. Ballester, Estimation of unitary quantum operations, *Phys. Rev. A* **69**, 022303 (2004).
  - [25] Z. Hou, J.-F. Tang, J. Shang, H. Zhu, J. Li, Y. Yuan, K.-D. Wu, G.-Y. Xiang, C.-F. Li, and G.-C. Guo, Deterministic realization of collective measurements via photonic quantum walks, *Nat. Commun.* **9**, 10.1038/s41467-018-03849-x (2018).
  - [26] Y. Yuan, Z. Hou, J.-F. Tang, A. Streltsov, G.-Y. Xiang, C.-F. Li, and G.-C. Guo, Direct estimation of quantum coherence by collective measurements, *Npj Quantum Inf.* **6**, 10.1038/s41534-020-0280-6 (2020).
  - [27] L. O. Conlon, F. Eilenberger, P. K. Lam, and S. M. Assad, Discriminating mixed qubit states with collective measurements, *Commun. Phys.* **6**, 10.1038/s42005-023-01454-z (2023).
  - [28] K. Matsumoto, A new approach to the Cramér-Rao-type bound of the pure-state model, *J. Phys. A* **35**, 3111–3123 (2002).
  - [29] C. Helstrom, Minimum mean-squared error of estimates in quantum statistics, *Phys. Lett. A* **25**, 101–102 (1967).
  - [30] C. Helstrom, The minimum variance of estimates in quantum signal detection, *IEEE Trans. Inf. Theory* **14**, 234 (1968).
  - [31] A. S. Holevo, *Probabilistic and Statistical Aspects of Quantum Theory* (Springer, 2011).
  - [32] H. Nagaoka, A new approach to Cramér-Rao bounds for quantum state estimation, in *Asymptotic Theory of Quantum Statistical Inference* (World Scientific, 2005) p. 100–112.
  - [33] H. Nagaoka, A generalization of the simultaneous diagonalization of Hermitian matrices and its relation to quantum estimation theory, in *Asymptotic Theory of Quantum Statistical Inference* (World Scientific, 2005) p. 133–149.
  - [34] J. Kahn and M. Guță, Local asymptotic normality for finite dimensional quantum systems, *Commun. Math. Phys.* **289**, 597–652 (2009).
  - [35] K. Yamagata, A. Fujiwara, and R. D. Gill, Quantum local asymptotic normality based on a new quantum likelihood ratio, *Ann. Stat.* **41**, 2197 (2013).
  - [36] Y. Yang, G. Chiribella, and M. Hayashi, Attaining the ultimate precision limit in quantum state estimation, *Commun. Math. Phys.* **368**, 223–293 (2019).
  - [37] B. Li, L. O. Conlon, P. K. Lam, and S. M. Assad, Optimal single-qubit tomography: Realization of locally optimal measurements on a quantum computer, *Phys. Rev. A* **108**, 032605 (2023).
  - [38] M. Gell-Mann, Symmetries of Baryons and Mesons, *Phys. Rev.* **125**, 1067 (1962).
  - [39] Y. Watanabe, T. Sagawa, and M. Ueda, Uncertainty relation revisited from quantum estimation theory, *Phys. Rev. A* **84**, 042121 (2011).
  - [40] J. Suzuki, Explicit formula for the Holevo bound for two-parameter qubit-state estimation problem, *J. Math. Phys.* **57**, 042201 (2016).
  - [41] F. Albarelli, J. F. Friel, and A. Datta, Evaluating the Holevo Cramér-Rao bound for multiparameter quantum metrology, *Phys. Rev. Lett.* **123**, 200503 (2019).
  - [42] L. O. Conlon, J. Suzuki, P. K. Lam, and S. M. Assad, The gap persistence theorem for quantum multiparameter estimation 10.48550/arxiv.2208.07386 (2022).
  - [43] M. Tsang, The Holevo Cramér-Rao bound is at most thrice the Helstrom version 10.48550/arxiv.1911.08359 (2019).
  - [44] A. Carollo, B. Spagnolo, A. A. Dubkov, and D. Valenti, On quantumness in multi-parameter quantum estimation, *J. Stat. Mech.: Theory Exp.* **2019** (9), 094010.
  - [45] L. O. Conlon, P. K. Lam, and S. M. Assad, Multiparameter estimation with two-qubit probes in noisy channels, *Entropy* **25**, 1122 (2023).
  - [46] L. O. Conlon, J. Suzuki, P. K. Lam, and S. Assad, *The Gap Persistence Theorem Between Nagaoka–Hayashi Bound and Holevo Bound for Quantum Multiparameter Estimation*, Tech. Rep. 123, 14 (IEICE, 2023).
  - [47] M. Hayashi and Y. Ouyang, Tight Cramér-Rao type bounds for multiparameter quantum metrology through conic programming, *Quantum* **7**, 1094 (2023).
  - [48] R. A. Bertlmann and P. Krammer, Bloch vectors for qudits, *J. Phys. A* **41**, 235303 (2008).
  - [49] J. Suzuki, Information geometrical characterization of quantum statistical models in quantum estimation theory, *Entropy* **21**, 10.3390/e21070703 (2019).
  - [50] A. Fujiwara and H. Nagaoka, An estimation theoretical characterization of coherent states, *J. Math. Phys.* **40**, 4227–4239 (1999).
  - [51] G. M. D’Ariano, L. Maccone, and M. G. A. Paris, Quorum of observables for universal quantum estimation, *J. Phys. A* **34**, 93–103 (2000).
  - [52] G. M. D’Ariano, P. Perinotti, and M. F. Sacchi, Informationally complete measurements and group representation, *J. Opt. B: Quantum Semiclass. Opt.* **6**, S487–S491 (2004).
  - [53] D. R. Cox and N. Reid, Parameter orthogonality and approximate conditional inference, *J. R. Stat. Soc., B* **49**, 1 (1987).

- [54] A. Candeloro, Z. Pazhotan, and M. G. A. Paris, Dimension matters: precision and incompatibility in multi-parameter quantum estimation models [10.48550/arxiv.2403.07106](https://arxiv.org/abs/10.48550/arxiv.2403.07106) (2024).
- [55] H. E. Haber, Useful relations among the generators in the defining and adjoint representations of  $SU(N)$ , *SciPost Phys. Lect. Notes*, **21** (2021).
- [56] V. I. Borodulin, R. N. Rogalyov, and S. R. Slabospitskii, *Core 3.2 (compendium of relations, version 3.2)* (2022), [arXiv:1702.08246 \[hep-ph\]](https://arxiv.org/abs/1702.08246).
- [57] A. E. Rastegin, Uncertainty relations for MUBs and SIC-POVMs in terms of generalized entropies, *Eur. Phys. J. D* **67**, 269 (2013).
- [58] G. Tóth and I. Apellaniz, Quantum metrology from a quantum information science perspective, *J. Phys. A* **47**, 424006 (2014).

### Appendix A: Gell-Mann Matrices and Tomography via Parameter Estimation

The main advantage of the Bloch representation for qubits,

$$\rho = \frac{1}{2} \left( \mathbb{1}_2 + \sum_{j \in \{x, y, z\}} \theta_j \sigma_j \right), \quad (\text{A1})$$

where  $\mathcal{P} := \{\sigma_x, \sigma_y, \sigma_z\}$  is the Pauli basis, is the convenience of working with the real-valued Bloch vector  $\theta := \{\theta_x, \theta_y, \theta_z\} \in \mathbb{R}^3$  instead of the equivalent complex operator  $\rho \in \mathbb{C}^{2 \times 2}$ . The same convenience is availed in three dimensions by replacing  $\mathcal{P}$  with the GMMs,  $\Lambda_3 := \{\lambda_j\}_{j=1}^8$ . These constitute an orthonormal basis over the reals for the space of  $3 \times 3$  traceless Hermitian matrices and generalise the Pauli matrices to three dimensions. So for a qutrit state  $\rho$ , we can write

$$\rho = \mathbb{1}_3/3 + \sum_{j=1}^8 \theta_j \lambda_j \quad (\text{A2})$$

with

$$\begin{aligned} \lambda_1 &= \frac{1}{\sqrt{2}} \begin{bmatrix} 0 & 1 & 0 \\ 1 & 0 & 0 \\ 0 & 0 & 0 \end{bmatrix}, & \lambda_2 &= \frac{1}{\sqrt{2}} \begin{bmatrix} 0 & -i & 0 \\ i & 0 & 0 \\ 0 & 0 & 0 \end{bmatrix}, \\ \lambda_3 &= \frac{1}{\sqrt{2}} \begin{bmatrix} 1 & 0 & 0 \\ 0 & -1 & 0 \\ 0 & 0 & 0 \end{bmatrix}, & \lambda_4 &= \frac{1}{\sqrt{2}} \begin{bmatrix} 0 & 0 & 1 \\ 0 & 0 & 0 \\ 1 & 0 & 0 \end{bmatrix}, \\ \lambda_5 &= \frac{1}{\sqrt{2}} \begin{bmatrix} 0 & 0 & -i \\ 0 & 0 & 0 \\ i & 0 & 0 \end{bmatrix}, & \lambda_6 &= \frac{1}{\sqrt{2}} \begin{bmatrix} 0 & 0 & 0 \\ 0 & 0 & 1 \\ 0 & 1 & 0 \end{bmatrix}, \\ \lambda_7 &= \frac{1}{\sqrt{2}} \begin{bmatrix} 0 & 0 & 0 \\ 0 & 0 & -i \\ 0 & i & 0 \end{bmatrix}, & \lambda_8 &= \frac{1}{\sqrt{6}} \begin{bmatrix} 1 & 0 & 0 \\ 0 & 1 & 0 \\ 0 & 0 & -2 \end{bmatrix}. \end{aligned} \quad (\text{A3})$$

Note that we choose a different convention in Eq. (A2) from that in Eq. (A1), and we set  $\text{Tr}(\lambda_j \lambda_k) = \delta_{jk}$  instead of the standard  $2\delta_{jk}$  in Eq. (A3) for convenience.

The eight GMMs in Eq. (A3) for  $d = 3$  can be extended to  $d > 3$  leading to the generalised GMMs  $\Lambda_d$  (that we shall also refer to as GMMs). In fact,  $\Lambda_d$  consists of  $\binom{d}{2}$  real, symmetric matrices that generalise  $\sigma_x$ ,  $\binom{d}{2}$  imaginary, skew-symmetric matrices that generalise  $\sigma_y$ , and  $d - 1$  real, diagonal matrices that generalise  $\sigma_z$ . In total, we have  $d^2 - 1$  matrices,  $\{\lambda_j\}_{j=1}^{d^2-1}$ , in  $\Lambda_d$ , and, for arbitrary qudit density matrix  $\rho$  in  $d$  dimensions, we can write

$$\rho = \mathbb{1}_d/d + \sum_{j=1}^{d^2-1} \theta_j \lambda_j \quad (\text{A4})$$

to get a one-to-one map between  $\rho \leftrightarrow \theta$ . Resultantly, a qudit state estimation or tomography problem can be treated as a parameter estimation problem with  $\theta$  as the unknown parameter. Note that our convention in Eq. (A4) is different from that used in some existing literature [48] but is equivalent up to a re-scaling of the parameters, which leaves the ratio unchanged.

### Appendix B: Proof of Generalised Gell-Mann Matrix Identities

In this appendix, we prove the following identities for  $\Lambda_d = \{\lambda_j\}_{j=1}^{d^2-1}$ .

1.  $\sum_{j \in [n]} \lambda_j^2 = \frac{d^2-1}{d} \mathbb{1}_d$
2.  $\sum_{m \in [n]} \lambda_m \lambda_j \lambda_m = -\frac{1}{d} \lambda_j$
3.  $\sum_{j, k \in [n]} \lambda_j \lambda_k \lambda_j \lambda_k = -\frac{d^2-1}{d^2} \mathbb{1}_d$

*Proof of Identity 1.* It is known that  $\sum_{j \in [n]} \lambda_j^2$  is a group invariant called the Casimir operator [55]. Thus,  $\sum_{j \in [n]} \lambda_j^2 = C \mathbb{1}_d$  for some constant  $C$ . We use the trace condition  $\text{Tr}(\lambda_j \lambda_k) = \delta_{jk}$

$$\text{Tr} \left( \sum_{j \in [n]} \lambda_j^2 \right) = \sum_{j \in [n]} \text{Tr}(\lambda_j^2) = n = Cd, \quad (\text{B1})$$

which implies  $C = n/d$ , proving

$$\sum_{j \in [n]} \lambda_j^2 = \frac{d^2-1}{d} \mathbb{1}_d.$$

□

*Proof of Identity 2.* For this proof, we use some properties of GMMs from Ref. [56] (see page 17, Sec. 4.6 *Gell-Mann Matrices in n-dimensions*). Writing the product  $\lambda_m \lambda_j$  in terms of the commutator and the anti-commutator, we get

$$\begin{aligned} 2\lambda_m \lambda_j &= \{\lambda_m, \lambda_j\} + [\lambda_m, \lambda_j] \\ &= \frac{2}{d} \delta_{mj} \mathbb{1}_d + \sum_c d_{mjc} \lambda_c + \sum_c i f_{mjc} \lambda_c, \end{aligned} \quad (\text{B2})$$



where  $d_{jkl} = \text{Tr}(\{\lambda_j, \lambda_k\}\lambda_l)$  and  $f_{jkl} = -i \text{Tr}([\lambda_j, \lambda_k]\lambda_l)$  are the fully-symmetric and fully-antisymmetric structure constants<sup>9</sup> of  $\mathfrak{su}(d)$  [55, 56]. Repeating the process after right-multiplying Eq. (B2) by  $\lambda_m$ ,

$$\begin{aligned}
2\lambda_m \lambda_j \lambda_m &= \frac{2}{d} \delta_{mj} \lambda_m + \sum_c (d_{mjc} + i f_{mjc}) \lambda_c \lambda_m \\
&= \frac{2}{d} \delta_{mj} \lambda_m + \frac{1}{2} \sum_c (d_{mjc} + i f_{mjc}) \left( \frac{2}{d} \delta_{cm} \mathbf{1}_d \right. \\
&\quad \left. + \sum_p (d_{cmp} + i f_{cmp}) \lambda_p \right) \\
&= \frac{2}{d} \delta_{mj} \lambda_m + \frac{1}{d} (d_{mjm} + i f_{mjm}) \mathbf{1}_d \\
&\quad + \frac{1}{2} \sum_{c,p} (d_{mjc} + i f_{mjc}) (d_{cmp} + i f_{cmp}) \lambda_p
\end{aligned} \tag{B3}$$

Due to anti-symmetry,  $f_{mjm} = 0$ , and

$$\begin{aligned}
&(d_{mjc} + i f_{mjc})(d_{cmp} + i f_{cmp}) \\
&= [(d_{mjc} d_{cmp} - f_{mjc} f_{cmp}) \\
&\quad + i(d_{mjc} f_{cmp} + f_{mjc} d_{cmp})].
\end{aligned} \tag{B4}$$

Thus,

$$\sum_m \lambda_m \lambda_j \lambda_m = \frac{1}{d} \lambda_j + \frac{1}{2d} \underbrace{\sum_m d_{mjm} \mathbf{1}_d}_{\textcircled{1}} \tag{B5}$$

$$+ \frac{1}{4} \sum_p \left[ \underbrace{\sum_{m,c} d_{mjc} d_{cmp}}_{\textcircled{2}} - \underbrace{\sum_{m,c} f_{mjc} f_{cmp}}_{\textcircled{3}} \right] \tag{B6}$$

$$+ i \left( \underbrace{\sum_{m,c} d_{mjc} f_{cmp}}_{\textcircled{4}} + \underbrace{\sum_{m,c} f_{mjc} d_{cmp}}_{\textcircled{5}} \right) \lambda_p. \tag{B7}$$

Below we evaluate terms  $\textcircled{1}, \textcircled{2}, \textcircled{3}, \textcircled{4}$  and  $\textcircled{5}$  one by one, using properties of the GMMs listed in Ref. [56].

$$\begin{aligned}
\textcircled{1}: \sum_m d_{mjm} &= \sum_m d_{jmm} \\
&= \frac{1}{4} \text{Tr} \left[ \lambda_j \sum_m \{\lambda_m, \lambda_m\} \right] = \frac{1}{2} \text{Tr} \left[ \lambda_j \frac{d^2 - 1}{d} \mathbf{1}_d \right] \\
&= \frac{d^2 - 1}{2d} \text{Tr}(\lambda_j) = 0
\end{aligned} \tag{B8}$$

$$\textcircled{2}: \sum_{m,c} d_{mjc} d_{cmp} = \sum_{m,c} d_{jmc} d_{pmc} = 2 \frac{d^2 - 4}{d} \delta_{jp} \tag{B9}$$

$$\textcircled{3}: \sum_{m,c} f_{mjc} f_{cmp} = \sum_{m,c} f_{jmc} f_{pmc} = 2d \delta_{jp} \tag{B10}$$

The Jacobi identity [56] reads

$$\sum_k d_{abk} f_{kcl} + d_{bck} f_{kal} + d_{cak} f_{kbl} = 0.$$

If we set  $a = c$  and then sum over  $a$ , we get

$$2 \sum_{a,k} d_{bak} f_{lak} = \sum_k \left( \sum_a d_{aak} \right) f_{blk}.$$

Using this to simplify  $\textcircled{4}$ , we get

$$\textcircled{4}: \sum_{m,c} d_{mjc} f_{cmp} = - \sum_{m,c} d_{jmc} f_{pmc} = - \frac{1}{2} \sum_{m,c} d_{mmc} f_{jpc} \tag{B11}$$

and, similarly, for  $\textcircled{5}$  we get

$$\begin{aligned}
\textcircled{5}: \sum_{m,c} f_{mjc} d_{cmp} &= - \sum_{m,c} d_{pmc} f_{jmc} \\
&= - \frac{1}{2} \sum_{m,c} d_{mmc} f_{pjc} = \frac{1}{2} \sum_{m,c} d_{mmc} f_{jpc},
\end{aligned} \tag{B12}$$

so that

$$\textcircled{4} + \textcircled{5}: \sum_{m,c} (d_{mjc} f_{cmp} + f_{mjc} d_{cmp}) = 0. \tag{B13}$$

Combining the expressions for  $\textcircled{1}, \textcircled{2}$  and  $\textcircled{3}$ , we get

$$\begin{aligned}
\sum_m \lambda_m \lambda_j \lambda_m &= \frac{1}{d} \lambda_j + \frac{1}{4} \sum_p \left( 2 \frac{d^2 - 4}{d} - 2d \right) \delta_{jp} \lambda_p \\
&= \frac{1}{d} \lambda_j - \frac{2}{d} \lambda_j = - \frac{1}{d} \lambda_j,
\end{aligned} \tag{B14}$$

thus proving Identity 2.  $\square$

*Corollary 1.* By linearity, any  $d \times d$  traceless Hermitian matrix  $A$  satisfies

$$\sum_m \lambda_m A \lambda_m = - \frac{1}{d} A. \tag{B15}$$

*Corollary 2.* For any  $j, k \in [n]$ ,

$$\sum_m \lambda_m \lambda_j \lambda_k \lambda_m = \delta_{jk} \mathbf{1}_d - \frac{1}{d} \lambda_j \lambda_k. \tag{B16}$$

<sup>9</sup> Owing to different normalisation conventions, our  $d_{abc}$  and  $f_{abc}$  are scaled up by a factor of  $\sqrt{2}$  compared to Ref. [56].

*Proof.* To see this, start with assuming  $j \neq k$ . From Eq. (B2), this implies  $\lambda_j \lambda_k$  is traceless Hermitian, and thus from Corollary 1,

$$\sum_m \lambda_m \lambda_j \lambda_k \lambda_m = -\frac{1}{d} \lambda_j \lambda_k.$$

Similarly, for  $j = k$ ,  $\lambda_j \lambda_k - \frac{1}{d} \mathbb{1}_d$  is a traceless, Hermitian matrix (see Eq. (B2)). Thus, from Corollary 1,

$$\sum_m \lambda_m \left( \lambda_j^2 - \frac{1}{d} \mathbb{1}_d \right) \lambda_m = -\frac{1}{d} \left( \lambda_j^2 - \frac{1}{d} \mathbb{1}_d \right),$$

so that

$$\sum_m \lambda_m \lambda_j^2 \lambda_m = \mathbb{1}_d - \frac{1}{d} \lambda_j^2. \quad (\text{B17})$$

This concludes the proof of Corollary 2.  $\square$

*Proof of Identity 3.* Using Identity 2, we have

$$\sum_j \lambda_j \lambda_k \lambda_j \lambda_k = \left( \sum_j \lambda_j \lambda_k \lambda_j \right) \lambda_k = -\frac{1}{d} \lambda_k^2. \quad (\text{B18})$$

Summing over  $k$  and using Identity 1, we find

$$\sum_{j,k} \lambda_j \lambda_k \lambda_j \lambda_k = -\frac{1}{d} \sum_k \lambda_k^2 = -\frac{d^2 - 1}{d^2} \mathbb{1}_d, \quad (\text{B19})$$

which proves Identity 3.  $\square$

### Appendix C: Deferred Proofs: Proof of Lemma 1

*Proof of Lemma 1.* The proof is segmented into three parts. (i) First we establish that the  $X_j$  are completely and uniquely determined by the local unbiasedness conditions to be  $X_j = \lambda_j$ . This can be traced back to the trace orthonormality  $\text{Tr}[\lambda_j \lambda_k] = \delta_{jk}$  of GMMs. (ii) We establish a lower bound on  $C_{\text{HCRB}}$ . (iii) We show this lower bound is achieved by valid choices of arguments  $\mathbb{S}_\theta$  and  $\mathbb{L}$ , implying  $C_{\text{HCRB}}$  is equal to the lower bound.

*Part (i):* The local unbiased conditions

$$\text{Tr}[\rho_\theta X_j] = \theta_j \text{ and } \text{Tr}[\partial_j \rho_\theta X_k] = \delta_{jk} \quad (\text{C1})$$

for  $j, k \in [d^2 - 1]$  at  $\theta = 0$  become

$$\text{Tr}[X_j] = 0 \text{ and } \text{Tr}[\lambda_j X_k] = \delta_{jk}, \quad (\text{C2})$$

and are solved by  $X_j = \lambda_j$  as

$$\text{Tr}[\lambda_j] = 0 \text{ and } \text{Tr}[\lambda_j \lambda_k] = \delta_{jk}. \quad (\text{C3})$$

It is simple to verify that any other solution  $X_j$ , which by virtue of being traceless and Hermitian must be a linear combination of  $\lambda_k$ s as

$$X_j = \sum_k c_{j,k} \lambda_k \quad c_{j,k} \in \mathbb{C}, \quad (\text{C4})$$

has to satisfy  $\text{Tr}[\lambda_j X_k] = c_{k,j} = \delta_{jk}$ , so  $X_j = \lambda_j$ , leading to a contradiction.

*Part (ii):* Tracing over the parameter indices ( $\text{Tr}$ ) in

$$\text{Tr}[\mathbb{S}_\theta \mathbb{L}] \succcurlyeq \text{Tr}[\mathbb{S}_\theta \mathbb{X} \mathbb{X}^\top] \quad (\text{C5})$$

yields

$$\text{Tr}[\mathbb{S}_\theta \mathbb{L}] \geq \text{Tr}[\mathbb{S}_\theta \mathbb{X} \mathbb{X}^\top]. \quad (\text{C6})$$

*Remark 1.* The inequality in Eq. (C6) holds regardless of whether  $\mathbb{L} = \mathbb{X} \mathbb{X}^\top$  is a valid choice according to the constraints in Eq. (7). In the case where there is a unique set of LUB estimators  $\mathbb{X}$ , this reduces to  $C_{\text{HCRB}} \geq C_{\text{SLD}}$ . We utilise this fact in Sec. IV B, Appendix F, and Appendix G.

*Part (iii):* The choice  $\mathbb{L} = \mathbb{X} \mathbb{X}^\top$  leads to

$$(\text{Tr}[\mathbb{S}_\theta \mathbb{L}])_{j,k} = \text{Tr}[\mathbb{1}/d \lambda_j \lambda_k] = \delta_{jk}/d, \quad (\text{C7})$$

which is real, symmetric and has trace (over parameter indices)

$$\text{Tr}[\mathbb{S}_\theta \mathbb{L}] = \text{Tr}[\mathbb{S}_\theta \mathbb{X} \mathbb{X}^\top] = \frac{d^2 - 1}{d}. \quad (\text{C8})$$

Finally, from *part (ii)* we know that a lower  $\text{Tr}[\mathbb{S}_\theta \mathbb{L}]$  is not possible, thus proving Eq. (22).  $\square$

### Appendix D: SLD & RLD CRBs

The two simplest quantum Cramér-Rao bounds, the SLD and the RLD, generalise the logarithmic derivative of a parameterised probability distribution,

$$\partial_\theta p_\theta(x) = p_\theta(x) \partial_\theta [\log(p_\theta(x))] , \quad (\text{D1})$$

to linear operators acting on the density matrix  $\rho_\theta$ . The SLD version produces Hermitian operators  $\{L_j^{(\text{SLD})}\}$  and the RLD version produces operators  $\{L_j^{(\text{RLD})}\}$  defined implicitly via

$$2\partial_j \rho_\theta =: L_j^{(\text{SLD})} \rho_\theta + \rho_\theta L_j^{(\text{SLD})}, \quad (\text{D2})$$

$$\partial_j \rho_\theta =: \rho_\theta L_j^{(\text{RLD})}. \quad (\text{D3})$$

Once Eqs. (D2) and (D3) are solved for  $\{L_j^{(\text{SLD})}\}$  and  $\{L_j^{(\text{RLD})}\}$ , the corresponding QFIs can be computed using

$$[J^{(\text{SLD})}]_{jk} := \text{Re} \left[ \text{Tr} \left[ \rho_\theta L_j^{(\text{SLD})} L_k^{(\text{SLD})} \right] \right], \quad (\text{D4})$$

$$[J^{(\text{RLD})}]_{jk} := \text{Tr} \left[ \rho_\theta L_k^{(\text{RLD})} L_j^{(\text{RLD}) \dagger} \right]. \quad (\text{D5})$$

Notably,  $J^{(\text{SLD})}$  is real and symmetric and  $J^{(\text{RLD})}$  is complex and Hermitian. Finally, the traced versions of the

SLD and RLD QFI matrix inequalities  $V_\theta \succcurlyeq J^{(\text{SLD})^{-1}}$  and  $V_\theta \succcurlyeq J^{(\text{RLD})^{-1}}$  yield the scalar SLD and RLD CRBs

$$\text{Tr}(V_\theta) \geq C_{\text{SLD}} \quad \& \quad \text{Tr}(V_\theta) \geq C_{\text{RLD}}, \quad (\text{D6})$$

with

$$C_{\text{SLD}} = \text{Tr} \left[ J^{(\text{SLD})^{-1}} \right], \quad (\text{D7})$$

$$C_{\text{RLD}} = \text{Tr} \left[ \text{Re} \left[ J^{(\text{RLD})} \right]^{-1} \right] + \left\| \text{Im} \left[ J^{(\text{RLD})} \right]^{-1} \right\|_1, \quad (\text{D8})$$

where  $\|X\|_1 := \text{Tr}(\sqrt{X^\dagger X})$  denotes the trace norm. The SLD and RLD CRBs are not attainable in general, especially in multi-parameter contexts. For more details on the SLD and RLD CRB, see Ref. [13].

For the model in Sec. IV A,  $\rho_\theta^* = \mathbb{1}_d/d$  and  $\partial_j \rho_\theta = \lambda_j$ , so Eqs. (D2) & (D3) become

$$\begin{aligned} 2\lambda_j &= 2/d L_j^{\text{SLD}}, \\ \lambda_j &= 1/d L_j^{\text{RLD}} \end{aligned} \quad (\text{D9})$$

implying  $L_j^{\text{SLD}} = L_j^{\text{RLD}} = d\lambda_j$ . A direct computation of Eqs. (D4), (D5), (D7) & (D8) then yields the QFIs

$$J^{(\text{SLD})} = J^{(\text{RLD})} = \begin{bmatrix} d & 0 & \dots & 0 \\ 0 & d & \dots & \vdots \\ \vdots & \vdots & \ddots & 0 \\ 0 & \dots & 0 & d \end{bmatrix}_{n \times n}, \quad (\text{D10})$$

and the scalar CRBs

$$C_{\text{SLD}} = C_{\text{RLD}} = \frac{d^2 - 1}{d}, \quad (\text{D11})$$

as in main text Eqs. (19) and (20).

## Appendix E: Deferred Proofs: Proof of Lemma 2

### 1. SDP Formulation and Dual Problem

The SDP formulation of the NHCRB [19] is

$$C_{\text{NHCRB}} := \min_{\mathbb{Y}} \left[ \text{Tr}[\mathbb{F}_0 \mathbb{Y}] | \text{Tr}[\mathbb{F}_k \mathbb{Y}] = c_k, \mathbb{F}_0 = \begin{pmatrix} \mathbb{S}_\theta & 0 \\ 0 & 0 \end{pmatrix}, \right. \\ \left. \mathbb{Y} \geq 0 \right], \quad (\text{E1})$$

where  $\mathbb{F}_k$  are constant matrices and  $c_k$  are constants, as defined in Ref. [19] (supplementary note 4). The dual problem to the SDP in Eq. (E1) reads

$$\tilde{C}_{\text{NHCRB}} := \max_y \left[ \sum_k y_k c_k | \sum_k y_k \mathbb{F}_k \leq \mathbb{F}_0 \right]. \quad (\text{E2})$$

In the following two lemmas, we present solutions to the primal and dual problems.

**Lemma 3.** *The optimal  $\mathbb{L}$  for the primal problem in Eq. (4) is*

$$\mathbb{L}_{jk}^* = d+1/d+2 (\{\lambda_j, \lambda_k\} + \delta_{jk} \mathbb{1}_d) \quad (\text{E3})$$

where  $j, k \in [n]$  and  $\{\lambda_j, \lambda_k\}$  is the anti-commutator.

**Lemma 4.** *The optimal  $y$  for the dual problem in Eq. (E2),  $y^*$ , is such that*

$$\sum_k y_k^* \mathbb{F}_k = \begin{bmatrix} 0 & \mathbb{G}_{12}^{(1)} & \dots & \mathbb{G}_{1n}^{(1)} & \mathbb{G}_1^{(2)} \\ \mathbb{G}_{21}^{(1)} & 0 & \dots & \mathbb{G}_{2n}^{(1)} & \vdots \\ \vdots & \vdots & \ddots & \mathbb{G}_{(n-1)n}^{(1)} & \\ \mathbb{G}_{n1}^{(1)} & \dots & \mathbb{G}_{n(n-1)}^{(1)} & 0 & \mathbb{G}_n^{(2)} \\ \mathbb{G}_1^{(2)} & \dots & & \mathbb{G}_n^{(2)} & \mathbb{G}^{(3)} \end{bmatrix} \quad (\text{E4})$$

with

$$\begin{aligned} \mathbb{G}_{jk}^{(1)} &= -1/d [\lambda_j, \lambda_k] \\ \mathbb{G}_j^{(2)} &= d+1/d \lambda_j \\ \mathbb{G}^{(3)} &= -(d^2-1)(d+1)/d^2 \mathbb{1}_d, \end{aligned} \quad (\text{E5})$$

where  $j, k \in [n]$  and  $[\lambda_j, \lambda_k]$  is the commutator.

The proof of Lemmas 3 and 4 is broken up into the following three subsections. In Subsec. E2, we prove the feasibility of  $\mathbb{L}^*$  from Lemma 3. In Subsec. E3 we prove the feasibility of  $y^*$  from Lemma 4. Finally in Subsec. E4 we prove that the primal-objective value from  $\mathbb{L}^*$  equals the dual objective value from  $y^*$ , thus establishing their optimality and proving Lemma 2 from the main text.

### 2. Feasibility of $\mathbb{L}^*$ for the Primal Problem

The  $\mathbb{L}_{jk}^*$  from Lemma 3 is easily seen to be symmetric in  $j$  and  $k$ , meaning  $\mathbb{L}_{jk}^* = \mathbb{L}_{kj}^*$ .  $\mathbb{L}_{jk}^*$  is also seen to be Hermitian. To show  $\mathbb{L}^*$  is feasible, it only remains to show  $\mathbb{L}^* - \mathbb{X}\mathbb{X}^\top \geq 0$ . Writing  $\mathbb{L}^* - \mathbb{X}\mathbb{X}^\top$  as a block matrix,

$$\begin{aligned} (\mathbb{L}^* - \mathbb{X}\mathbb{X}^\top)_{jk} &= \frac{d+1}{d+2} (\{\lambda_j, \lambda_k\} + \delta_{jk} \mathbb{1}_d) - \lambda_j \lambda_k \\ &= \frac{d+1}{d+2} (\delta_{jk} \mathbb{1}_d + \mathbb{N}_{1jk} - \mathbb{N}_{2jk}) \end{aligned} \quad (\text{E6})$$

we see that we need to prove  $\mathbb{N} := \mathbb{1}_{nd} + \mathbb{N}_1 - \mathbb{N}_2 \geq 0$ , where we have defined block matrices

$$(\mathbb{N}_1)_{jk} := \lambda_k \lambda_j \quad \& \quad (\mathbb{N}_2)_{jk} := \frac{\lambda_j \lambda_k}{d+1}.$$

We first evaluate  $(\mathbb{N}_1 - \mathbb{N}_2)^2 = \mathbb{N}_1^2 + \mathbb{N}_2^2 - \mathbb{N}_1\mathbb{N}_2 - \mathbb{N}_2\mathbb{N}_1$  to find

$$\begin{aligned} (\mathbb{N}_1^2)_{jk} &= \delta_{jk} \mathbb{1}_d - 1/d \lambda_j \lambda_k \\ (\mathbb{N}_2^2)_{jk} &= \frac{d-1}{d(d+1)} \lambda_j \lambda_k \\ (\mathbb{N}_1\mathbb{N}_2)_{jk} &= -\frac{1}{d(d+1)} \lambda_j \lambda_k \\ (\mathbb{N}_2\mathbb{N}_1)_{jk} &= -\frac{1}{d(d+1)} \lambda_j \lambda_k, \end{aligned} \quad (\text{E7})$$

where we have used the identities proven in Appendix B. Combining these results we arrive at  $((\mathbb{N}_1 - \mathbb{N}_2)^2)_{jk} = \delta_{jk} \mathbb{1}_d$  which means  $(\mathbb{N}_1 - \mathbb{N}_2)^2 = \mathbb{1}_{nd}$ . From this, and using that  $\mathbb{N}_1 - \mathbb{N}_2$  is Hermitian, we can conclude that the eigenvalues of  $\mathbb{N}_1 - \mathbb{N}_2$  are  $\pm 1$ . Hence the eigenvalues of  $\mathbb{N} = \mathbb{1}_{nd} + \mathbb{N}_1 - \mathbb{N}_2$  are 0 and 2. This proves that  $\mathbb{N}$  is a positive semi-definite operator, and that  $\mathbb{L}^* - \mathbb{X}\mathbb{X}^\top \geq 0$ .  $\square$

### 3. Feasibility of $y^*$ for the Dual Problem

We need to show that the matrix  $\sum_k y_k^* \mathbb{F}_k$ , which explicitly is

$$\begin{bmatrix} 0 & \frac{1}{d}[\lambda_2, \lambda_1] & \dots & \frac{1}{d}[\lambda_n, \lambda_1] & \frac{d+1}{d} \lambda_1 \\ \frac{1}{d}[\lambda_1, \lambda_2] & 0 & \dots & \frac{1}{d}[\lambda_n, \lambda_2] & \vdots \\ \vdots & \vdots & \ddots & \frac{1}{d}[\lambda_n, \lambda_{n-1}] & \vdots \\ \frac{1}{d}[\lambda_1, \lambda_n] & \dots & \frac{1}{d}[\lambda_{n-1}, \lambda_n] & 0 & \frac{d+1}{d} \lambda_n \\ \frac{d+1}{d} \lambda_1 & \dots & \dots & \frac{d+1}{d} \lambda_n & -\frac{n(d+1)}{d^2} \mathbb{1}_d \end{bmatrix} \quad (\text{E8})$$

satisfies  $\mathbb{F}_0 - \sum_k y_k^* \mathbb{F}_k \geq 0$ . Note that this  $\sum_k y_k^* \mathbb{F}_k$  corresponds to  $y_j^*$  values

$$y_j^{(1)} = 0, \quad y_j^{(2)} = \frac{d+1}{d} \delta_{jk}, \quad y_j^{(3)} = 0 \quad (\text{E9})$$

$$y_{jkl}^{(4)} = -f_{jkl}/d, \quad y_j^{(5)} = -\frac{n(d+1)}{d\sqrt{d}} \delta_{j1} \quad (\text{E10})$$

whereas the corresponding  $c_j$  values are

$$c_j^{(1)} = 0, \quad c_j^{(2)} = 2\delta_{jk}, \quad c_j^{(3)} = 0 \quad (\text{E11})$$

$$c_{jkl}^{(4)} = 0, \quad c_j^{(5)} = \sqrt{d} \delta_{j1} \quad (\text{E12})$$

so that the dual objective value is

$$\sum_j 2y_{jj}^{(2)} + \sqrt{d}y_j^{(5)} = \frac{2n(d+1)}{d} - \frac{n(d+1)}{d} = \frac{n(d+1)}{d}. \quad (\text{E13})$$

To show this  $y^*$  is feasible, note that proving  $\mathbb{F}_0 - \sum_k y_k^* \mathbb{F}_k \geq 0$  is equivalent to showing

$$\begin{bmatrix} \mathbb{1}_d & [\lambda_1, \lambda_2] & \dots & [\lambda_1, \lambda_n] & -(d+1)\lambda_1 \\ [\lambda_2, \lambda_1] & \mathbb{1}_d & \dots & [\lambda_2, \lambda_n] & \vdots \\ \vdots & \vdots & \ddots & [\lambda_{n-1}, \lambda_n] & \vdots \\ [\lambda_n, \lambda_1] & \dots & [\lambda_n, \lambda_{n-1}] & \mathbb{1}_d & -(d+1)\lambda_n \\ -(d+1)\lambda_1 & \dots & \dots & -(d+1)\lambda_n & \frac{n(d+1)}{d} \mathbb{1}_d \end{bmatrix}$$

is positive semi-definite. Using Schur's complement lemma, this can be simplified to showing

$$\begin{bmatrix} \mathbb{1}_d & [\lambda_1, \lambda_2] & \dots & [\lambda_1, \lambda_n] \\ [\lambda_2, \lambda_1] & \mathbb{1}_d & \dots & [\lambda_2, \lambda_n] \\ \vdots & \vdots & \ddots & \vdots \\ [\lambda_n, \lambda_1] & \dots & [\lambda_n, \lambda_{n-1}] & \mathbb{1}_d \end{bmatrix} - \frac{d}{d-1} \begin{bmatrix} \lambda_1^2 & \lambda_1 \lambda_2 & \dots & \lambda_1 \lambda_n \\ \lambda_2 \lambda_1 & \ddots & \dots & \vdots \\ \vdots & \vdots & \ddots & \vdots \\ \lambda_n \lambda_1 & \lambda_n \lambda_2 & \dots & \lambda_n^2 \end{bmatrix} \geq 0 \quad (\text{E14})$$

We rewrite the left hand side of Eq. (E14) in the block-matrix representation as

$$\begin{aligned} & \delta_{jk} \mathbb{1}_d + [\lambda_j, \lambda_k] - \frac{d}{d-1} \lambda_j \lambda_k \\ &= \delta_{jk} \mathbb{1}_d - \frac{1}{d-1} \lambda_j \lambda_k - \lambda_k \lambda_j \\ &= (\mathbb{1}_{nd})_{jk} - \left( (\mathbb{M}_1)_{jk} + (\mathbb{M}_2)_{jk} \right), \end{aligned}$$

where we have defined

$$(\mathbb{M}_1)_{jk} := \frac{1}{d-1} \lambda_j \lambda_k \quad \& \quad (\mathbb{M}_2)_{jk} := \lambda_k \lambda_j. \quad (\text{E15})$$

Thus, we finally need to prove the following theorem to establish the feasibility of  $y^*$ .

**Theorem 4.** *The operator  $\mathbb{M} := \mathbb{1}_{nd} - (\mathbb{M}_1 + \mathbb{M}_2)$  is positive semi-definite.*

Before we can prove Theorem 4, we first need to prove the following two lemmas.

**Lemma 5.**  $\mathbb{M}_1$  and  $\mathbb{M}_2$  commute, i.e.,  $\mathbb{M}_1\mathbb{M}_2 = \mathbb{M}_2\mathbb{M}_1$ .

*Proof.* Using Identity 2 from Appendix B, we have

$$\begin{aligned} (\mathbb{M}_1\mathbb{M}_2)_{jk} &= \sum_l (\mathbb{M}_1)_{jl} (\mathbb{M}_2)_{lk} = \frac{1}{d-1} \sum_l \lambda_j \lambda_l \lambda_k \lambda_l \\ &= \frac{1}{d-1} \lambda_j \left( \frac{-1}{d} \lambda_k \right) = -\frac{1}{d(d-1)} \lambda_j \lambda_k, \end{aligned} \quad (\text{E16})$$

whereas

$$\begin{aligned} (\mathbb{M}_2\mathbb{M}_1)_{jk} &= \sum_l (\mathbb{M}_2)_{jl} (\mathbb{M}_1)_{lk} = \frac{1}{d-1} \sum_l \lambda_l \lambda_j \lambda_l \lambda_k \\ &= \frac{1}{d-1} \left( \frac{-1}{d} \lambda_j \right) \lambda_k = -\frac{1}{d(d-1)} \lambda_j \lambda_k. \end{aligned} \quad (\text{E17})$$

Hence  $\mathbb{M}_1\mathbb{M}_2 = \mathbb{M}_2\mathbb{M}_1$ , which also implies that  $\mathbb{M}_1$  and  $\mathbb{M}_2$  share some eigenvectors.  $\square$

**Lemma 6.**  $\mathbb{M}_1 + \mathbb{M}_2$  satisfies  $(\mathbb{M}_1 + \mathbb{M}_2)^2 = \mathbb{1}_{nd}$  or, equivalently,

$$[(\mathbb{M}_1 + \mathbb{M}_2)^2]_{jk} = \delta_{jk} \mathbb{1}_d$$

where  $j, k \in [n]$ .



*Proof.*

$$\begin{aligned}
& [(\mathbb{M}_1 + \mathbb{M}_2)^2]_{jk} \\
&= \sum_l (\mathbb{M}_1 + \mathbb{M}_2)_{jl} (\mathbb{M}_1 + \mathbb{M}_2)_{lk} \\
&= \sum_l \left( \frac{1}{d-1} \lambda_j \lambda_l + \lambda_l \lambda_j \right) \left( \frac{1}{d-1} \lambda_l \lambda_k + \lambda_k \lambda_l \right) \\
&= \frac{1}{(d-1)^2} \lambda_j \left( \sum_l \lambda_l^2 \right) \lambda_k + \sum_l \lambda_l \lambda_j \lambda_k \lambda_l \\
&+ \frac{1}{d-1} \left[ \lambda_j \left( \sum_l \lambda_l \lambda_k \lambda_l \right) + \left( \sum_l \lambda_l \lambda_j \lambda_l \right) \lambda_k \right]
\end{aligned}$$

so using Corollary 2 and Identities 1 and 2,

$$\begin{aligned}
&= \delta_{jk} \mathbb{1}_d + \left( \frac{d^2 - 1}{d(d-1)^2} - \frac{1}{d} - \frac{1}{d(d-1)} - \frac{1}{d(d-1)} \right) \lambda_j \lambda_k \\
&= \delta_{jk} \mathbb{1}_d.
\end{aligned}$$

□

Now we can prove Theorem 4 as follows.

*Proof of Theorem 4.* From Lemma 6, the eigenvalues of  $(\mathbb{M}_1 + \mathbb{M}_2)^2$  must all be 1. As  $(\mathbb{M}_1 + \mathbb{M}_2)$  is Hermitian, its eigenvalues must be  $\pm 1$ . It follows that the eigenvalues of  $\mathbb{M} = \mathbb{1}_{nd} - (\mathbb{M}_1 + \mathbb{M}_2)$  must be either 2 or 0. Hence  $\mathbb{M}$ , being a Hermitian matrix with non-negative eigenvalues, must be positive semi-definite. □

#### 4. Optimality of Solutions & Proof of Lemma 2

*Proof of Lemma 2.* Note that, by direct calculation,

$$\text{Tr}(\mathbb{S}_\theta \mathbb{L}^*) = \sum_k y_k^* c_k = \frac{(d^2 - 1)(d + 1)}{d}. \quad (\text{E18})$$

In other words,  $\mathbb{L}^*$  is primal-feasible and  $y^*$  is dual-feasible and the primal value equals the dual value. This lets us conclude that  $(d^2 - 1)(d + 1)/d$  is the true optimal value of the primal and dual problems, and that  $\mathbb{L}^*$  and  $y^*$  are optimal solutions to the primal and dual problems, respectively. As a result, we have

$$\text{C}_{\text{NHCRB}} = \frac{(d^2 - 1)(d + 1)}{d}. \quad (\text{E19})$$

□

#### 5. Attainability of NHCRB via SIC POVMs

**Lemma 7.** *The CFI matrix for estimating all GMMs from the maximally-mixed state  $\rho_m$  by measuring the SIC*

*POVM in  $d$  dimensions is*

$$J = \begin{bmatrix} \frac{d}{d+1} & 0 & \cdots & 0 \\ 0 & \frac{d}{d+1} & \cdots & 0 \\ \vdots & \vdots & \ddots & \vdots \\ 0 & 0 & \cdots & \frac{d}{d+1} \end{bmatrix}_{n \times n}. \quad (\text{E20})$$

*Proof of Lemma 7.* In the multi-parameter case, the CFI matrix  $J_{jk}$  ( $j, k \in [n]$ ) is given by

$$J_{jk}[\{\Pi_l\}] = \sum_{m=1}^{d^2} \frac{\text{Tr}[\partial_j \rho_\theta \Pi_m] \text{Tr}[\partial_k \rho_\theta \Pi_m]}{\text{Tr}[\rho_\theta \Pi_m]}, \quad (\text{E21})$$

From [57] we have that for any (rank-one) SIC POVM  $\{\Pi_m\}_{m=1}^{d^2}$ ,

$$\sum_{m=1}^{d^2} \text{Tr}[\rho \Pi_m]^2 = \frac{\text{Tr}[\rho^2] + 1}{d(d+1)} \quad (\text{E22})$$

for arbitrary density matrix  $\rho$ . For the diagonal elements in Eq. (E21), substituting  $\rho = \mathbb{1}/d + \theta_j \lambda_j$  into Eq. (E22) and using  $\text{Tr}(\rho^2) = 1/d + \theta_j^2$  gives

$$J_{jj} = d^2 \sum_{m=1}^{d^2} \text{Tr}[\lambda_j \Pi_m]^2 = \frac{d}{d+1}, \quad (\text{E23})$$

whereas for the off-diagonal elements, substituting  $\rho = \mathbb{1}/d + \theta_j \lambda_j + \theta_k \lambda_k$  into Eq. (E22) and using  $\text{Tr}(\rho^2) = 1/d + \theta_j^2 + \theta_k^2$  gives

$$J_{jk} = d^2 \sum_{m=1}^{d^2} \text{Tr}[\lambda_j \Pi_m] \text{Tr}[\lambda_k \Pi_m] = 0 \quad (j \neq k), \quad (\text{E24})$$

thus proving Eq. (E20). □

#### Appendix F: Estimating a Subset of GMMs

Consider estimating a subset  $\{\lambda_j\}_{j \in K}$  of GMMs from the maximally-mixed state  $\rho_m$ . Here  $K$  denotes a subset of  $n$  indices from 1 to  $n_{\max}$  ( $K \subseteq [n_{\max}]$ ,  $|K| = n$ ). Now, the corresponding unbiased estimators can be written as

$$X_j = \lambda_j + \sum_{m \in [n_{\max}] \setminus K} c_{jm} \lambda_m, \quad j \in K, c_{jm} \in \mathbb{R}, \quad (\text{F1})$$

which follows from the unbiasedness conditions in Eq. (17). Specifically,  $\text{Tr}(\partial_j \rho_\theta X_k) = \text{Tr}(\lambda_j X_k) = \delta_{jk}$  forces each  $X_j$  to contain a unit contribution from  $\lambda_j$  due to the orthonormality of the GMMs and  $\text{Tr}(\rho_\theta X_j) = \theta_j$  implies the only other GMMs contributing to  $X_j$  must be the ones not being estimated.

Notice that at the block-matrix level, this can be rewritten as

$$\mathbb{X} = \begin{bmatrix} \mathbb{1}_n & \mathbb{C}_{n \times (n_{\max} - n)}^{(1)} \end{bmatrix}_{n \times n_{\max}} \Lambda_d, \quad (\text{F2})$$

where  $\mathbb{X} := [X_1, \dots, X_n]^\top$ ,  $\Lambda_d := [\lambda_1, \dots, \lambda_{n_{\max}}]^\top$  and  $\mathbb{C}_{ab}^{(1)} = c_{ab}$ . For convenience, we also define

$$\mathbb{C}^{(2)} := \left[ \mathbf{1}_n \mid \mathbb{C}_{n \times (n_{\max} - n)}^{(1)} \right]_{n \times n_{\max}} \quad (\text{F3})$$

so that  $\mathbb{X}\mathbb{X}^\top = \mathbb{C}^{(2)}\Lambda_d\Lambda_d^\top\mathbb{C}^{(2)\top}$ .

We can now use the lower bound  $C_{\text{HCRB}} \geq \text{Tr}[\mathbb{S}_\theta \mathbb{X}\mathbb{X}^\top]$  from Remark 1 to get

$$C_{\text{HCRB}} \geq \frac{1}{d} \left( n + \sum_{a,b} (\mathbb{C}_{ab}^{(1)})^2 \right) \geq \frac{n}{d}. \quad (\text{F4})$$

Moreover, as in Appendix C,  $\mathbb{L} = \mathbb{X}\mathbb{X}^\top$  is a valid choice leading to

$$(\text{Tr}[\mathbb{S}_\theta \mathbb{L}])_{j,k} = \frac{1}{d} \left( \delta_{jk} + \sum_{l \in [n_{\max}] \setminus K} \mathbb{C}_{jl}^{(1)} \mathbb{C}_{kl}^{(1)} \right), \quad (\text{F5})$$

which is real, symmetric and gives  $\text{Tr}[\mathbb{S}_\theta \mathbb{L}] = \text{Tr}[\mathbb{S}_\theta \mathbb{X}\mathbb{X}^\top]$ . This proves

$$C_{\text{HCRB}} = \frac{n}{d} \quad (\text{F6})$$

following the same arguments as Appendix C. For estimating all  $n_{\max}$  parameters this reduces to Lemma 1. Numerical checks also verify this result, as shown, e.g., in Table I.

Notice that  $\Lambda_d\Lambda_d^\top$  is the same as  $\mathbb{X}\mathbb{X}^\top$  from Lemma 3, so that, using the fact that  $\mathbb{C}^{(2)\top}\mathbb{C}^{(2)} \succcurlyeq 0$ , we can modify  $\mathbb{L}^*$  from Lemma 3 as

$$\mathbb{L}^{**}(\mathbb{C}^{(1)}) := \mathbb{C}^{(2)}\mathbb{L}^*\mathbb{C}^{(2)\top}. \quad (\text{F7})$$

It then follows from Lemma 3 that

$$\begin{aligned} \mathbb{L}^* - \Lambda\Lambda^\top &\succcurlyeq 0 \\ \implies \mathbb{C}^{(2)}(\mathbb{L}^* - \Lambda\Lambda^\top)\mathbb{C}^{(2)\top} &\succcurlyeq 0 \\ \implies \mathbb{L}^{**} - \mathbb{X}\mathbb{X}^\top &\succcurlyeq 0. \end{aligned} \quad (\text{F8})$$

That this  $\mathbb{L}^{**}$  satisfies the other NHCRB constraints ( $\mathbb{L}_{jk}^{**} = \mathbb{L}_{kj}^{**}$  Hermitian from Eq. (4)) for all  $\mathbb{C}^{(1)}$  is also easy to check.

Note that  $C_{\text{NHCRB}}$  is now defined by the following minimisation:

$$\begin{aligned} C_{\text{NHCRB}} &:= \min_{\mathbb{L}, \mathbb{C}^{(1)}} \left\{ \text{Tr}[\mathbb{S}_\theta \mathbb{L} \mid \mathbb{L}_{jk} = \mathbb{L}_{kj} \text{ Hermitian}, \right. \\ &\quad \left. \mathbb{L} \succcurlyeq [\mathbf{1}_n \mid \mathbb{C}^{(1)}] \Lambda\Lambda^\top [\mathbf{1}_n \mid \mathbb{C}^{(1)}]^\top \right\}, \end{aligned} \quad (\text{F9})$$

whereas if we restrict the minimisation over  $\mathbb{L}$  to a minimisation over our ansatz  $\mathbb{L}^{**}(\mathbb{C}^{(1)})$ , we should get a

larger value than  $C_{\text{NHCRB}}$ , i.e.,

$$\begin{aligned} &\min_{\mathbb{L}, \mathbb{C}^{(1)}} \left\{ \text{Tr}[\mathbb{S}_\theta \mathbb{L} \mid \mathbb{L}_{jk} = \mathbb{L}_{kj} \text{ Hermitian}, \right. \\ &\quad \left. \mathbb{L} \succcurlyeq [\mathbf{1}_n \mid \mathbb{C}^{(1)}] \Lambda\Lambda^\top [\mathbf{1}_n \mid \mathbb{C}^{(1)}]^\top \right\} \\ &\leq \min_{\mathbb{C}^{(1)}} \left\{ \text{Tr}[\mathbb{S}_\theta \mathbb{L}^{**} \mid \mathbb{L}_{jk}^{**} = \mathbb{L}_{kj}^{**} \text{ Hermitian}, \right. \\ &\quad \left. \mathbb{L}^{**} \succcurlyeq [\mathbf{1}_n \mid \mathbb{C}^{(1)}] \Lambda\Lambda^\top [\mathbf{1}_n \mid \mathbb{C}^{(1)}]^\top \right\}. \end{aligned} \quad (\text{F10})$$

This is because the minimisation on the RHS of Eq. (F10) is over a subset of the set over which the minimisation on the LHS is performed. The quantity on the RHS of Eq. (F10) can then be simplified to

$$\min_{\mathbb{C}^{(1)}} \left\{ \frac{d+1}{d} \left( n + \sum_{a,b} (\mathbb{C}_{ab}^{(1)})^2 \right) \right\} = \frac{(d+1)n}{d}.$$

This lets us upper-bound  $C_{\text{NHCRB}}$  as

$$C_{\text{NHCRB}} \leq \frac{(d+1)n}{d}, \quad (\text{F11})$$

which for estimating all  $n_{\max}$  parameters reduces to Eq. (31) from Subsec. IV B. Combining with  $C_{\text{HCRB}} = n/d$ , we find

$$\frac{C_{\text{NHCRB}}}{C_{\text{HCRB}}} \leq d+1, \quad (\text{F12})$$

as claimed in Theorem 3. Numerically, we see this ratio actually depends on  $n$ : as  $n$  increases up to  $n_{\max}$ , the ratio increases up to  $d+1$ . Table I lists out  $C_{\text{HCRB}}$ ,

# parameters	$C_{\text{HCRB}}$	Range: $C_{\text{NHCRB}}$	Max Ratio
2	2/3	(2/3, 4/3)	2
3	1	(3/2, 3)	3
4	4/3	(2.85, 4.0834)	3.0625
5	5/3	(25/6, 5.4352)	3.2611
6	2	(6, 7.0922)	3.5461
7	7/3	(8.437, 8.495)	3.6408
8	8/3	32/3	4

TABLE I. HCRB and NHCRB for estimating a subset  $\{\lambda_j\}_{j \in K} \subseteq \Lambda_3$  of GMMs for the maximally-mixed qutrit state. The HCRB depends only on the number of parameters,  $|K|$ , but the NHCRB depends on the subset  $K$  chosen, so we tabulate its range in the third column, as (Min NHCRB, Max NHCRB). The fourth column lists the maximum ratio between the NHCRB and the HCRB, taking into account all possible subsets  $\{\lambda_j\}_{j \in K}$ .

the minimum and maximum values of  $C_{\text{NHCRB}}$  and the maximum ratio for estimating a given number of GMMs on qutrits. The HCRB only depends on  $n$  but not on which GMMs are chosen and is equal to  $n/d$ .

## Appendix G: Extension to Arbitrary Weight Matrices

In this section, we extend the ratio bound of  $d + 1$  for the linear GMM model to arbitrary parameter-independent full-rank weight matrices  $W$ . For fair comparison with the unweighted case, corresponding to  $W = \mathbb{1}_n$ , we trace-normalise  $\text{Tr}(W) = n$ . Additionally,  $W$  must be real, symmetric, and positive semi-definite ( $W \succcurlyeq 0$ ). This weighted model then corresponds to reparameterisations of the linear GMM model [13, 19, 50], i.e., estimating any  $n_{\max}$  parameters that are not necessarily coefficients of the GMMs. Similar to the other cases where all  $n_{\max}$  parameters are estimated, the unbiased estimators are uniquely fixed to be  $X_j = \lambda_j$ . We first bound the weighted HCRB, and then the weighted NHCRB, to prove the ratio is at most  $d + 1$  for the maximally-mixed case. Then, to extend to arbitrary states, we numerically demonstrate that for fixed  $W$ , the ratio for  $\rho_m$  is always larger than the ratio for any other  $\rho_\theta$  but we do not give a proof.

The weighted HCRB is defined via [41]

$$C_{\text{HCRB}}^W[\rho_\theta] := \min_{\substack{V \in \mathbb{R}^{n \times n}, \\ V = V^\top}} \{ \text{Tr}[WV] \mid V \succcurlyeq \mathbb{Z}_\theta[\mathbb{X}] \}, \quad (\text{G1})$$

where, by explicit computation for the maximally-mixed case,  $\mathbb{Z}_\theta[\mathbb{X}]_{jk} = \text{Tr}[\rho_m X_j X_k] = \delta_{jk}/d$  or  $\mathbb{Z}_\theta[\mathbb{X}] = 1/d \mathbb{1}_n$ . Then, it follows from the positivity of  $W$  that  $V \succcurlyeq 1/d \mathbb{1}_n$  implies

$$WV \succcurlyeq \frac{1}{d}W \implies \text{Tr}[WV] \geq \text{Tr}[W]/d = \frac{n}{d}. \quad (\text{G2})$$

This proves  $C_{\text{HCRB}}^W[\rho_m] \geq n/d$ .

The weighted NHCRB is defined via [19]

$$C_{\text{NHCRB}}^W[\rho_\theta] := \min_{\mathbb{L}} \left\{ \text{Tr}[WV] \mid V = \text{Tr}[\mathbb{S}_\theta \mathbb{L}] \right. \\ \left. \mathbb{S}_\theta = \mathbb{1}_n \otimes \rho_\theta, \mathbb{L}_{jk} = \mathbb{L}_{kj} \text{ Hermitian}, \right. \\ \left. \mathbb{L} \succcurlyeq \mathbb{X}\mathbb{X}^\top \right\}. \quad (\text{G3})$$

Notably, the feasibility constraints on  $\mathbb{L}$  are unchanged from the unweighted case, i.e., the optimal  $\mathbb{L}^*$  from Lemma 3 still satisfies  $\mathbb{L}_{jk}^* = \mathbb{L}_{kj}^*$  Hermitian and  $\mathbb{L}^* \succcurlyeq \mathbb{X}\mathbb{X}^\top$ , despite not being optimal for the minimisation in Eq. (G3). This sub-optimal  $\mathbb{L}^*$  thus yields an upper bound to the minimum in Eq. (G3),

$$C_{\text{NHCRB}}^W[\rho_m] \leq \text{Tr} \left[ W \text{Tr} \left[ \frac{1}{d} \mathbb{1}_{nd} \mathbb{L}^* \right] \right] \\ = \frac{d+1}{d} \text{Tr}[W] = \frac{n(d+1)}{d}, \quad (\text{G4})$$

which proves  $C_{\text{NHCRB}}^W[\rho_m] \leq n(d+1)/d$ . Combining with  $C_{\text{HCRB}}^W[\rho_m] \geq n/d$  then proves the claim,

$$\frac{C_{\text{NHCRB}}^W[\rho_m]}{C_{\text{HCRB}}^W[\rho_m]} \leq d+1. \quad (\text{G5})$$

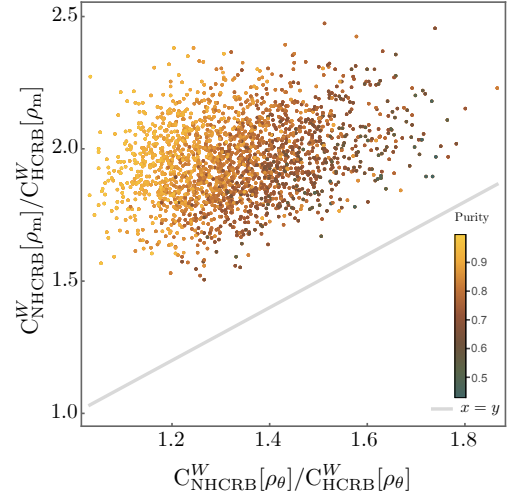


FIG. 4. Comparison of the weighted ratio  $C_{\text{NHCRB}}^W/C_{\text{HCRB}}^W$  for arbitrary states  $\rho_\theta$  to the equally-weighted ratio for the maximally-mixed state  $\rho_m$ , for the full-parameter linear GMM model (5000 samples). The points are colour-coded by the purity of  $\rho_\theta$  and the grey line corresponds to  $y = x$ .

So far, in this weighted tomography setting, which is equivalent to full tomography in arbitrary basis, we have established the ratio to be at most  $d + 1$  only for the maximally-mixed state. We do not prove the bound for arbitrary states but numerically demonstrate its validity in Fig. 4. By generating random full-rank, real, symmetric and positive  $W$ , such that  $\text{Tr}(W) = n$ , and random full-rank states  $\rho_\theta$ , we compare the ratio  $C_{\text{NHCRB}}^W[\rho_m]/C_{\text{HCRB}}^W[\rho_m]$  to the ratio  $C_{\text{NHCRB}}^W[\rho_\theta]/C_{\text{HCRB}}^W[\rho_\theta]$ . Repeating this over 5000 random samples of  $W$  and  $\rho_\theta$ , we find the weighted ratio for  $\rho_m$  to always be larger than the equally-weighted ratio for the maximally-mixed state. This means

$$\frac{C_{\text{NHCRB}}^W[\rho_\theta]}{C_{\text{HCRB}}^W[\rho_\theta]} \leq \frac{C_{\text{NHCRB}}^W[\rho_m]}{C_{\text{HCRB}}^W[\rho_m]} \leq d+1, \quad (\text{G6})$$

thus establishing the upper bound of  $d + 1$  for arbitrary full-parameter estimation from any state.

## Appendix H: Gill-Massar Cramér-Rao Bound

An alternative proof that the SIC POVM constitutes an individual-optimal measurement can be established via Gill-Massar's inequality for individual measurements [21],

$$\text{Tr}[J^{(\text{SLD})-1} J] \leq d-1. \quad (\text{H1})$$

For the SLD QFI  $J^{(\text{SLD})}$  in Eq. (19), the inequality in Eq. (H1) implies that  $\text{Tr}(J^{-1}) \geq (d^2 - 1)(d + 1)/d$ , which is saturated by the SIC POVM CFI  $J$  from Eq. (27), as seen in Eq. (28). In fact, the Gill-Massar Cramér-Rao bound (GMCrb) [21], obtained from Eq. (H1) by inserting the classical CRB from Eq. (2), is identical to the

NHCRB for the full-parameter linear GMM model. This follows from the inequality in Eq. (H1) being saturated in this case (Sec. VC below Eq. (54) in [21]). We further numerically verify this equivalence in Fig. 5, where we plot the two bounds for estimating all 8 GMM coefficients from 2000 random qutrit states. Both bounds agree for this case, as evidenced by the points all lying on the  $y = x$  line. However, this equivalence raises the question of why we choose the NHCRB over the GMCRB as our main tool to quantify finite-copy precision, which we now answer.

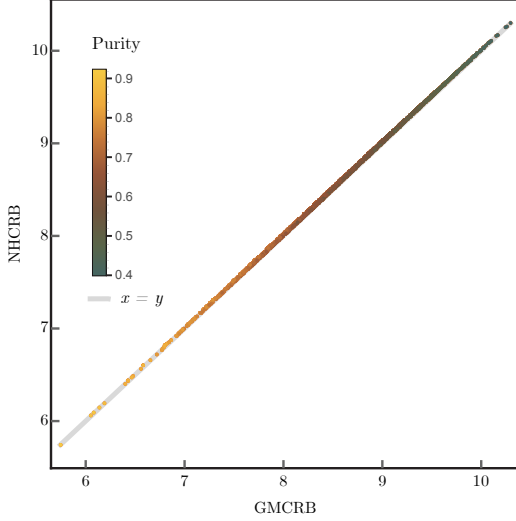


FIG. 5. Comparison of the NHCRB and the GMCRB for tomography in the GMM basis ( $n = 8$ ,  $d = 3$ ). The two bounds are equal for the 2000 randomly-generated states and are color-coded by purity of the state.

In short, the NHCRB is a tighter bound than the GMCRB in many cases of interest, and has a sub-additive

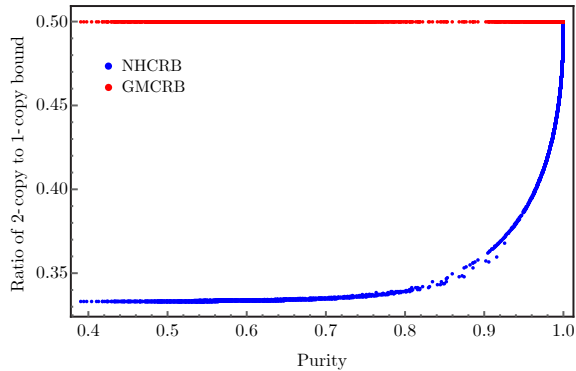


FIG. 6. Comparison of the two-copy to one-copy ratio for the NHCRB and the GMCRB. Bounds correspond to tomography in the GMM basis ( $n = 8$ ,  $d = 3$ ) for 5000 random states. The GMCRB is additive and underestimates the two-copy enhancement except for pure states, where the two bounds agree and there is no two-copy enhancement.

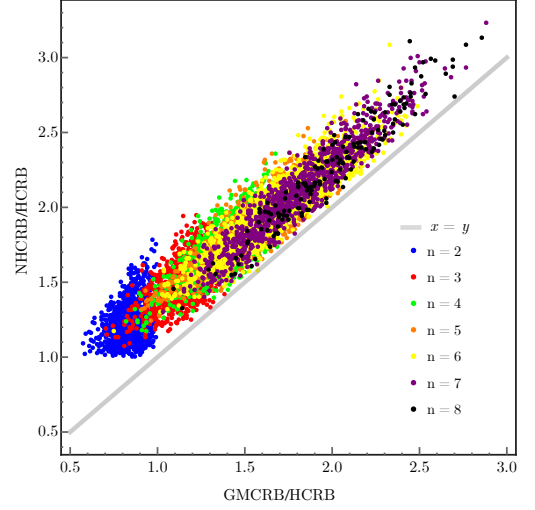


FIG. 7. Comparison of the NHCRB and the GMCRB, normalised by the HCRB, for estimating fewer than  $n_{\max}$  parameters via individual measurements. The bounds are calculated for 2000 random qutrit states with number of parameters  $n$  ranging from two to eight. The NHCRB is tighter than the GMCRB for this model.

scaling with number of copies similar to  $C_{\text{MI}}$ , whereas the GMCRB is additive with number of copies. The multi-copy GMCRB [21] is defined via

$$C_{\text{GMCRB}}[\rho_{\theta}^{\otimes k}] := \min_{V_{\theta}^{(k)} \succcurlyeq 0} \left\{ \left| \text{Tr}(V_{\theta}^{(k)}) \right| \right. \\ \left. \text{Tr}(J_{\text{SLD}}^{-1}(kV_{\theta}^{(k)})^{-1}) \leq d - 1 \right\}, \quad (\text{H2})$$

where  $^{(k)}$  represents  $k$ -copy quantities. Rephrasing the minimisation in Eq. (H2) in terms of  $kV_{\theta}^{(k)}$  directly leads to

$$C_{\text{GMCRB}}[\rho_{\theta}^{\otimes k}] = \frac{1}{k} C_{\text{GMCRB}}[\rho_{\theta}], \quad (\text{H3})$$

meaning the GMCRB is additive for measuring  $k$  copies of  $\rho_{\theta}$  simultaneously. This complements the well-known additivity of the SLD QFI (Eqs. (72) & (73) in [58]), on which the GMCRB is based.

For  $k = 2$ , Eq. (H3) implies that the ratio of the two-copy bound to the one-copy bound is exactly half for the GMCRB, as can be seen in Fig. 6. In Fig. 6, we compare the ratio of two-copy to one-copy bounds for the NHCRB and the GMCRB over 5000 randomly generated qutrit states. It is clear that the NHCRB is not additive with respect to number of copies; instead, the two-copy NHCRB is always smaller than the two-copy GMCRB, except for pure states where the two bounds agree. This subadditivity of the NHCRB and additivity of the GMCRB can be attributed to the fact that the  $k$ -copy GMCRB considers individually measuring each of the  $k$  copies, whereas the  $k$ -copy NHCRB considers measuring the  $k$ -copies simultaneously or collectively. As a



result, the gap between two-copy NHCRB and GMCRB represents the increase in precision from two-copy measurements compared to one-copy measurements. Notably the optimal Fisher information is also not additive under tensoring.

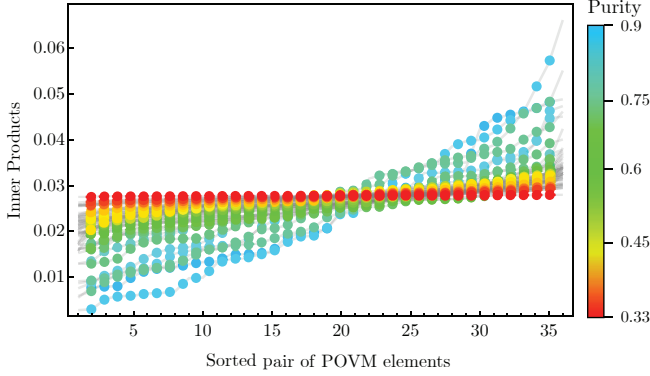


FIG. 8. Evolution of the qutrit individual-optimal measurements from SIC POVM (red) to IC POVMs (all other colours) as purity of  $\rho_\theta$  increases from  $1/3$  for the maximally-mixed state to  $1$  for pure states.

Moreover, for estimating fewer than  $n_{\max}$  parameters, the NHCRB is strictly higher than the GMCRB even in the one-copy case, i.e., the former is a tighter bound. Fig. 7 depicts this by considering the estimation of 2 to 8 arbitrary parameters from 2000 randomly generated qutrit states (following the same methodology as used in Fig. 3 to generate the states and parameters). The GMCRB and NHCRB are computed for this model and are both normalised by the HCRB. It is clear that all the plotted points lie above the  $y = x$  line, numerically demonstrating that the NHCRB is tighter than the GMCRB in this case. Nonetheless, Fig. 7 also reveals an increasing trend of the ratio between the individual-optimal and collective-optimal precisions with number of parameters, irrespective of the particular choice of the individual-precision bound.

#### Appendix I: Optimal IC POVMs for Arbitrary States

In this section we numerically investigate the optimal POVMs saturating the NHCRB for the full-parameter linear GMM model and for arbitrary states  $\rho_\theta^*$ . As the purity of  $\rho_\theta^*$  increases from  $1/d$  to  $1$ , the optimal individual measurements evolve from SIC POVMs to distorted IC POVMs. This transition is depicted in Fig. 8, where the inner products between the POVM vectors are equal at minimum purity but spread out with increasing purity. For Fig. 8, we first generate 500 random mixed qutrit states by uniformly-randomly choosing the parameters  $\{\theta_j\}$  and rejection-sampling to ensure the positivity of  $\rho_\theta$ . For each state, we numerically solve for the optimal one-copy,  $d^2$ -element, rank-one POVM and ensure that

it saturates the NHCRB. Then we compute the inner-product between every pair of elements of this optimal POVM. We then bin the states into 57 purity intervals and average the sorted list of inner products over each interval. Finally, we plot these sorted inner-products for each purity interval, colour-coded by the average purity of that interval.

#### Appendix J: Random-Sampling of States and Parameters

For the random-sampling experiments in Fig. 2, we generate random mixed qudit states by first generating an entry-wise random  $d \times d$  complex matrix  $S$ , and then assigning  $\rho_\theta = SS^\dagger / \text{Tr}(SS^\dagger)$ . This procedure ensures  $\rho_\theta = \rho_\theta^\dagger$ ,  $\rho_\theta \succcurlyeq 0$  and  $\text{Tr}(\rho_\theta) = 1$ . The true GMM coefficients ( $\theta^*$  for the GMM model) can be found via  $\text{Tr}(\rho_\theta \lambda_j)$ . Unfortunately, this procedure generates low-purity states with a much higher probability than high-purity states, which becomes a problem for  $d = 3$  and  $4$ . We circumvent this issue by generating additional samples by taking convex combinations of already-sampled states, which, despite making the sampling non-uniform, allows us to fully explore the region of allowed ratios for fixed purity. Specifically, for randomly-generated  $\rho_\theta$ , we consider the convex combinations  $(1 - p)\rho_\theta + p\mathbb{1}_d/d$  and  $(1 - p)\rho_\theta + p|+\rangle\langle +|_d$ , where  $(p \in [0, 1])$ . We compute the ratio for the full-parameter linear GMM model for all these states, the random samples and their convex combinations, to produce the yellow points in Fig. 2. The ratio-maximising (red) and -minimising states (blue) at fixed purity are found by numerically maximising and minimising the ratio over the state space.

For the random-sampling experiments in Figs. 3 and 9, we generate random mixed qudit states by the following technique. For each  $d$  and  $n$ , we uniformly-randomly choose  $n_{\max}$  coefficients  $\{\phi_j\}_{j \in [n_{\max}]}$  from the interval  $[-\sqrt{(d-1)/d}, \sqrt{(d-1)/d}]$ . These define a random state  $\rho_\theta = \mathbb{1}_d + \sum_{j \in [n_{\max}]} \phi_j \lambda_j$  which is guaranteed to be trace-one and Hermitian, but not positive. We ensure the positive semi-definiteness of  $\rho_\theta$  by rejection sampling (discarding if it is not positive). This process generates a valid random qudit state. Next we generate the  $n$  arbitrary parameters  $\{\theta_j\}_{j \in [n]}$  by generating at random the parameter derivatives  $\partial_j \rho_\theta$ , which must be Hermitian and traceless. We do this by writing each  $\partial_j \rho_\theta$  in the GMM basis and randomly generating the coefficients in this basis. Then we rejection-sample to ensure the  $n$  parameter derivatives are linearly-independent, and lead to a valid model.

Fig. 9 indicates that the  $10^4$  number of samples is relatively small for higher  $d$  and  $n$ —the minimum ratio observed, which should be close to one, is much larger for large  $d$  and  $n$ . This is because our sampling method generates states with low purity with higher probability and

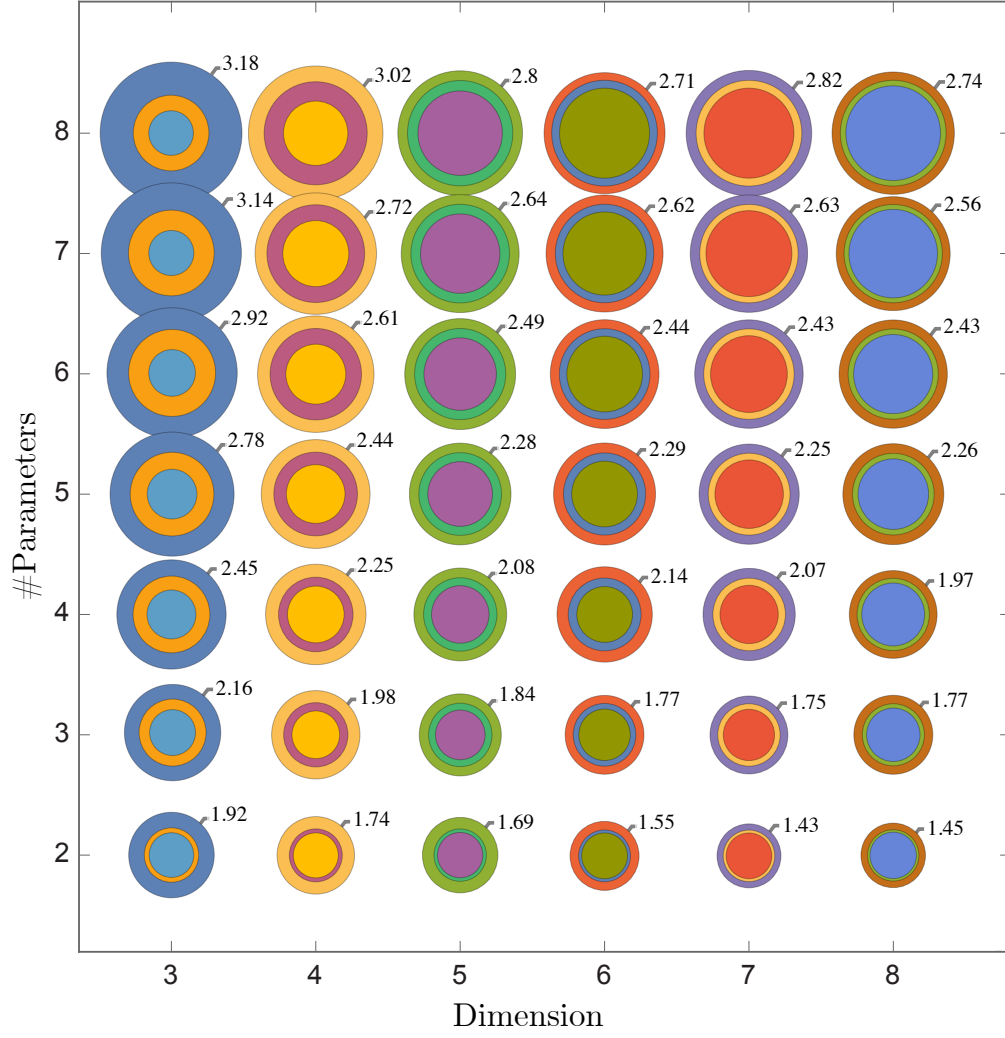


FIG. 9. Bubble plot of random sampling data for the ratio between the NHCRB and the HCRB for estimating arbitrary parameters from arbitrary qudit states. Bubbles are plotted on a grid over qudit dimension  $d$  and number of parameters  $n$ . The size (diameter) of the bubbles indicate the minimum, the average and the maximum ratios sampled for each  $d$  and  $n$ , and the numerical labels are the maximum ratio up to three significant figures.

states with high purity with lower probability. As a result, the increasing or decreasing trends of the maximum

observed ratio with  $n$  or  $d$  are not perfect for large  $d$  and  $n$  in Fig. 3.